Journal of Cleaner Production 447 (2024) 141394

Contents lists available at ScienceDirect

Journal of Cleaner Production

journal homepage: www.elsevier.com/locate/jclepro

HS3 as a novel solvent for carbon capture: Model validation and an industrial case study with comparison against 30 wt% MEA

Matteo Gilardi [a,b,*], Filippo Bisotti [a,**], Hanna K. Knuutila [c], Davide Bonalumi [b]

[a] SINTEF Industry – Process Technology, KPMT – Kjemisk Prosess Og Miljøteknologi, Richard Birkelands Vei 2A, 7034, Trondheim, Norway
[b] Politecnico di Milano- Department of Energy, Via Lambruschini 4A, 20156, Milano, Italy
[c] Department of Chemical Engineering, Norwegian University of Science and Technology, NTNU, Trondheim, NO-7491, Norway

ARTICLE INFO

Handling Editor: Jin-Kuk Kim

Keywords:
Amine blends
CO_2 capture
ELECNRTL aspen plus
Model validation
Process design and optimization
Energy integration

ABSTRACT

CO_2 capture is currently the most mature technological solution to reduce the environmental footprint of several emitters. However, the characterization of innovative blends with reduced energy demand and environmental impact is nowadays a challenge to increase the profitability and deployment of carbon capture on an industrial scale. This work investigates an innovative non-proprietary amine blend, called HS3. This article presents the development of a full model (including thermodynamics, kinetics, and mass transfer) and its validation with pilot-scale data covering temperature, CO_2 concentration, and capture rate ranges of interest for industrial applications. The model predicts the main process Key Performance Indicators, such as CO_2 captured, stripped flow, and cycling capacity, with deviations from the measurements lower than 7%. Then, the validated model is exploited for sizing and designing a carbon capture process from the flue gas generated within an oil refinery. A special focus is devoted to energy integration and process optimization by means of a sensitivity analysis. Eventually, HS3 performances are compared to benchmark MEA in terms of energy requirements and unit operation sizing for the same case study. Results show that HS3 can reduce the specific reboiler duty (MJ/kg CO_2 captured) and the required solvent flow per unit of flue gas (kg/kg) by 21% and 19%, respectively. Examples of comprehensive models developed starting from lab-scale testing up to the validation on a pilot scale are still limited in the literature. The validation in a semi-industrial pilot is needed to fully understand the solvent properties including, for instance, drawbacks which cannot be detected on a small scale. Needless to mention, reliable models are needed for consistent scale-up, techno-economic assessment, and LCA analysis. Thus, this present presents a model validation using semi-industrial pilot data and measurements, which is not common in the literature.

1. Introduction

1.1. The need for innovative solvents in carbon capture processes

The decarbonisation of several industrial sites is an essential step towards a net-zero emission scenario within the next 25 years (Emissions Gap Report, 2022). The emission cut is urgent both from stack/-point sources (Bui et al., 2018) and distributed source, such as air (Bisotti et al., 2023). To this aim, carbon capture from industrial flue gases and its storage or utilization is gaining interest as an option to significantly limit (Bui et al., 2018) and possibly make negative (Bisotti et al., 2024) the environmental impact associated with production sites generating flue gas streams, such as power plants, chemical industries, oil refineries, and steel/aluminium factories (Cachola et al., 2023). Although CO_2 absorption with amines is a mature technology, i.e., TRL 9 (Technology Readiness Level), its deployment is still limited due to the high energy demand (Bui et al., 2018) and numerous solvents have been tested to find solvent with high capacity and preferable vapor-liquid equilibrium behaviour (Bernhardsen and Knuutila). However, the latter is only one of the focuses when developing new solvents. Solvent degradation, corrosion, and the formation of harmful degradation products are also factors to be accounted for, as well as solvent make-up due to degradation and volatile solvent losses, i.e., additional costs for the reintegration of the losses, and impact on human health and the

* Corresponding author. SINTEF Industry – Process Technology, KPMT – Kjemisk Prosess Og Miljøteknologi, Richard Birkelands Vei 2A, 7034, Trondheim, Norway.
** Corresponding author.
E-mail addresses: matteo.gilardi@sintef.no (M. Gilardi), filippo.bisotti@sintef.no (F. Bisotti).

https://doi.org/10.1016/j.jclepro.2024.141394
Received 19 October 2023; Received in revised form 29 January 2024; Accepted 20 February 2024
Available online 27 February 2024

environment (Buvik et al., 2021). For this reason, developing new amines and amine blends with lower operating costs of the carbon capture process is necessary (Pellegrini et al., 2021).

1.2. HS3 solvent development

A new blend of 15 wt% 3-amino-1-propanol, (AP) and 30 wt% 1-2-hydroxyethyl-pyrrolydine (PRLD) was developed and characterized within the European projects HiPerCap, acronym for High Performance Capture (Kvamsdal et al., 2014), part of the FP7 programme (High Performance Capture, 2014) and REALISE (Demonstrating a Refinery, 2020),[1] an H2020 programme funded project. This blend combines the high CO_2 uptake capacity with a low energy-demanding regeneration with degradation stability similar to that of 30 wt% MEA (mono-ethanol amine). HiPerCap project (Kvamsdal et al., 2017) focused on, among other things, identifying an innovative solvents to overcome solvent-based carbon capture drawbacks and facilitate carbon capture deployment and defining an effective approach to screen amines and their blends to get reliable preliminary assessments of their performance and accelerate the development of a novel solvent technology from the lab to the industrial scale (Kim et al., 2019). In addition, the scope was to identify an alternative to non-proprietary CESAR1 solvent with ~20% less energy consumption per unit of mass of captured CO_2, and higher solvent stability compared to 30 wt% MEA (Moser et al., 2021). Several blends with strong bicarbonate-forming amine were tested in silico (Tobiesen et al., 2017) and experimentally (A. A Hartono et al., 2017). Eventually, the HiPerCap project came up with a blend of AP and PRLD as the most promising one to replace MEA. The identified blend of AP and PRLD has been reported to perform similary to CESAR1 solvent with 20% lower the thermal energy demand while increasing the cycling capacity, i.e., solvent recirculation reduced by 15% in mass compared to 30 wt% MEA (Tobiesen et al., 2017). Later, the formulation was further improved to minimize the energy demand (Hartono and Knuutila, 2021). The final optimized combination of 15 wt% AP and 30 wt% PRLD is called HS3. The findings are in-line with other works focusing on optimizing blends constituents and composition (Zhang et al., 2023a), i.e., the relative content of the active molecules, to reduce the energy demand (Chen et al., 2022). Moreover, other recent studies showed that the addition in the blend formulation of a strong bicarbonate-forming amine contributes to a drop of energy consumption (Zhang et al., 2023b).

HS3 solvent has already been extensively characterized on a laboratory scale in terms of vapor-liquid equilibria (VLE) and calorimetric measurements for both AP and PRLD blends (paper under preparation), analysis of the tertiary amine PRLD (A. Hartono et al., 2017) and additional physical properties such as viscosity and density for both pure amines and their mixtures (Hartono and Knuutila, 2023).

1.3. Structure of the present work

This work is split into two main parts with different tasks and objectives. The first part describes the implementation of a comprehensive model for the HS3 blend in Aspen Plus V11 and its validation using quality pilot-scale experimental data collected at SINTEF Tiller CO_2Lab. Pilot-scale data have been collected at SINTEF's Tiller pilot facility[2] with a full carbon capture pilot plant for two different CO_2 contents in the flue gas: 5.5 vol% and 12 vol%. Experimental observations showed that HS3 allows to operate with a lower solvent flow for a given flow of CO_2 to be treated ($kg_{solv}/kg_{CO2capt}$) compared to MEA solvent. Despite more concentrated (55 wt% amines against 30 wt% of MEA in water solution), HS3 lend regeneration is less energy-intensive. To address the potential of the solvent, the validation of the model is needed for the purpose of optimization of the design of a commercial-scale CO_2 capture plant, as well as for estimating energy requirements and cost assessment (Morgan et al., 2022).

Comparing the energy requirements, total costs, and emissions of an HS3 and an MEA CO_2 capture plant is one of the key steps to assess the new solvent's economic and environmental sustainability. Indeed, the solvent performance, e.g., CO_2 uptaking capacity and kinetic, directly influences the unit design, the energy consumption, and the overall capacity of the system. We decided to make a direct comparison with 30 wt% MEA as it is the current benchmark for solvent-based carbon capture (Feron et al., 2020). In other terms, when compared to first-generation amines such as MEA, second-generation blends such as CESAR and HS3 are supposed to reduce the energy consumption and total demand for amine recirculated in the system. This is reflected in a higher cycling capacity and lower liquid-gas ratios as discussed by Feron et al. for proprietary solvents (Feron et al., 2020) and Linag et al. for open-access ones (Liang et al., 2015).

The second part is a preliminary outlook on the process design, scale-up, and comparison with MEA amine system for a real industrial application. Indeed, the obtained model is applied on a refinery flue gas case study to assess the potentialities of HS3 for industrial-scale CO_2 capture, with a special focus on the potential for energy recovery strategies and process optimization. The proposed application is a key task of the EU H2020 REALISE project, where research institutes and industrial partners are connected to speed up innovative CCUS solutions development and pave the way for their large-scale deployment. The comparison between HS3 and reference MEA 30 wt% solvent is presented in terms of energy requirements, unit operations sizing, and the main key performance indicators.

1.4. Scope of the work and novelty

The present work gives an overview of model validation of a novel blend using semi-industrial pilot data, which is not common in the literature. Worldwide, there are still a few facilities used for testing carbon capture solvents until TRL-7 as at Tiller (Nessi et al., 2021). SINTEF's pilot plant (Mejdell et al., 2011) is one of the largest facilities for solvent testing before upscaling and pre-commercialization if compared to others listed in Nessi et al. The Technology Center Mongstad, known as TCM (Mongstad, Norway), Petra Nova (Texas, USA) and SaskPower's Boundary Dam (Saskatchewan, Canada) are larger facilities. Mongstad TCM is meant for industrial testing (Bui et al., 2020) while Petra Nova and Saskatchewan for demonstration (Mantripragada et al., 2019). During solvent development, validation in a relevant environment as pre-industrialization step (Buchner et al., 2019) is important.

Recent publications by Morgan et al. (2018) and Soares Chinen et al. (2019) proposed model validation on experimental data for MEA on different scales. Lee et al. investigated several innovative amine blends on a pilot scale, but these look to be proprietary solvents and they do not provide any details on the composition and constituents (Lee et al., 2019). Their analysis is limited to essential details for a single run of the experimental campaign without any detail in the column size, collected measurements in terms of methodology, number of samplings, and structure of the pilot (i.e., packing height and mesh). Conversely to prior literature, in the present work, we are proposing a detailed and transparent approach for model validation. Moreover, for the sake of transparency, we are publishing all the results from our analysis and the validation of the model is based on open-access data collected on a pilot plant. Finally, the present work is a preliminary assessment of the new solvent compared to MEA. The analysis is limited to energy demand (i.e., energy saving and main advantages).

[1] Project homepage - https://realiseccus.eu/.

[2] SINTEF CO_2Lab at Tiller - https://www.sintef.no/en/all-laboratories/co2-laboratory-tiller/.

2. Objectives and methods

2.1. General scope and objectives

This article deals with validation of the model for the HS3 blend in Aspen Plus V11.0. The Aspen process model uses Electrolyte Non-Random Two Liquid (ELECENRTL) thermodynamic model to describe the phase equilibrium, mass transfer (i.e., CO_2 diffusion into the solvent), and kinetics (i.e., chemical rate of the reactions occurring when CO_2 reacts with the amines). First, the vapor-liquid equilibrium (VLE) model has been fitted to lab-scale VLE data collected for the quaternary system AP-PRLD–CO_2–H_2O at the HS3 conposition between 40 °C and 120 °C. The procedure followed to develop the equilibrium model, as well as its testing on experimental data and a description of the system speciation in the liquid phase is described in detail in Gilardi et al. (2023). Here, we are providing the readers with the missing details. The kinetics for AP and PRLD reactions with CO_2 is proposed in accordance with the literature. The diffusion of CO_2 into the amine solutions have been estimated based on the liquid viscosity by means of the Wilke-Change method, for which a dedicated Aspen model has been tailored to experimental viscosity data using the Andrade model for mixtures. We present the validation of the proposed Aspen model by comparing its predictions with experimental pilot runs. The good accuracy and predictive capacity of the obtained model suggest its reliability for design and scale-up purposes, as well as energy demand and costs estimation on an industrial scale.

In the light of the promising validation outcomes, the proposed model is used to size, design, and optimize a large-scale application of interest for the REALISE H2020 EU project, namely the treatment of eight flue gas stacks generated by the Irving Whitegate oil refinery (Cork, Ireland). Operating parameters such as the solvent lean loading, the columns packing heights and the stripper pressure are selected based on the outcomes of a sensitivity analysis to find the optimal process design. For the sake of comparison with the benchmark solvent, the same CO_2 capture process has been simulated using the 30 wt% MEA Aspen Plus V11 default template available in Aspen Plus (Aspen Plus, 2019). The same process layout and the same methodology for process optimization have been followed for both solvents to guarantee the consistency for the comparison. A discussion on specific strategies for heat recovery within the plant to minimize the duty (steam) to be provided by an external heat source is addressed. Since internal heat recovery can only cover a fraction of the thermal heat demand for solvent regeneration, the residual steam is supposed to be generated on-site by means of a natural gas-fed boiler. The resulting flue gas from the steam generator is conveyed to the capture plant to reach the desired overall capture rate (90%). Eventually, HS3 and MEA performances for the Irving refinery case study are compared in terms of key performance indicators (KPIs) and energy requirements at assigned capture efficiency.

2.2. Methods: model development for rate-based simulations

2.2.1. Thermodynamic framework background (ELECNRTL)

HS3 solvent has been modelled in Aspen Plus® V11.0 by means of the Electrolyte Non-Random Two Liquids (ELECNRTL) model, where the activity coefficients account for the non-idealities in the liquid phase. This approach is an extension of the Non-Random Two Liquids (NRTL) framework (Renon and Prausnitz, 1969) to account for short and long-range interactions between cation-anion pairs with neutral molecules inside mixed solvents electrolyte systems in a wide temperature range (Hartono et al., 2021). This modification introduces the like-ion repulsion and local electro-neutrality assumptions (Lin et al., 2010) to provide a representative picture of the electrical charge effects. This is the most common approach to model amine systems in Aspen Plus® (Aspen Plus, 2019). The procedure set up and the regression of the short-range interactions of the ELECNRTL framework have been accomplished and described in a previous publication (Gilardi et al., 2023).

A short recap of the VLE model performance in predicting the partial pressure of CO_2 as a function of the loading and the heat of absorption is included in this section to highlight the reliability of the thermodynamic framework exploited as a background basis for the present work. Fig. 1A compares the partial pressure of CO_2 as a function of the loading as predicted by the developed Aspen VLE model-only (without kinetics and mass transfer) with respect to the experimental observations at different temperatures (40 °C, 60 °C, 80 °C, 100 °C and 120 °C). The proposed model underestimates the CO_2 partial pressure at 40 °C and very high loadings (>0.75 mol/mol) which is not of interest for a post-combustion process (Conway et al., 2014). However, there are no experimental data at high loadings for other temperatures to state that the model in general underestimates. Mono-functional amines such as AP and PRLD and their blends reach their maximum loading at around 0.40–0.60 (El Hadri et al., 2017), which is the equilibrium condition at the bottom of the absorber for conventional flue gas where the partial pressure of CO_2 (P_{CO2}) ranges from 3 to 15 kPa depending on the upstream combustion process and carbon source (Markewitz et al., 2012). In the domain of interest, e.g., loading from 0.05 to 0.55 and temperature between 40 °C and 120 °C, the thermodynamic model shows accuracy and good interpretation of the experimental data. Hence, despite missing experimental data, we are confident to extrapolate the model also at 122–125 °C, slightly higher temperatures registered at the reboiler during the Tiller campaign. These results will be corroborated in the validation as described and commented in the next sections.

The ELECNRTL model is sufficiently accurate in representing the equilibrium conditions in the whole investigated temperature and loading (0.1–0.5) range of interest for both absorption and regeneration. The profiles show quite smooth trends, allowing the model to be extrapolated outside the loadings range covered by experimental data. Reasonable AARD of 17.8 % and 17.0 % for CO_2 and H_2O partial pressures are obtained for 40, 60, 80, 100 and 120 °C, respectively. The average absolute error is 0.07 kPa for both partial pressures.

Fig. 1B and C report absorption heat profiles at temperatures of 60 °C and 100 °C. The monotonic decreasing profile shown by the Aspen model is realistic (seen with other blends earlier) and the fit is good considering the fluctuation in the experimental data. A statistical analysis covering a range from 40 °C to 100 °C shows that, even if the model slightly overestimates the heat released at high loadings at 40 °C, a sufficiently good agreement with the experimental data is observed in the whole loading and temperature range of interest. The calculated AARD are equal to 10.1%, 4.1%, 6.1% and 6.2% at 40 °C, 60 °C, 80 °C and 100 °C, respectively.

2.2.2. Kinetics

Reactions (1) and (2) describes the global reactions of the CO_2 capture based on the reactivity of the HS3 solvent constituents. These two reactions are the carbamate formation for primary amine (AP) and bicarbonate favoured by the tertiary amine (PRLD), respectively.

$$AP + H_2O + CO_2 \rightleftarrows APCOO^- + H_3O^+ \quad (1)$$

$$PRLD + H_2O + CO_2 \rightleftarrows PRLDH^+ + HCO_3^- \quad (2)$$

The kinetics are second-order rates and the velocity is defined in expression (3) as recommended in the literature (Penny and Ritter, 1983).

$$r = k_{R-dir} \cdot c_{Amine} \cdot c_{CO_2} \quad (3)$$

The reverse reactions rate, as in expression (4), is defined as the product of the kinetic constant time the concentration of the two reactants (R_1 and R_2) involved. These two compounds correspond to the product of the corresponding direct reaction:

$$r = k_{R-rev} \cdot c_{R1} \cdot c_{R2} \quad (4)$$

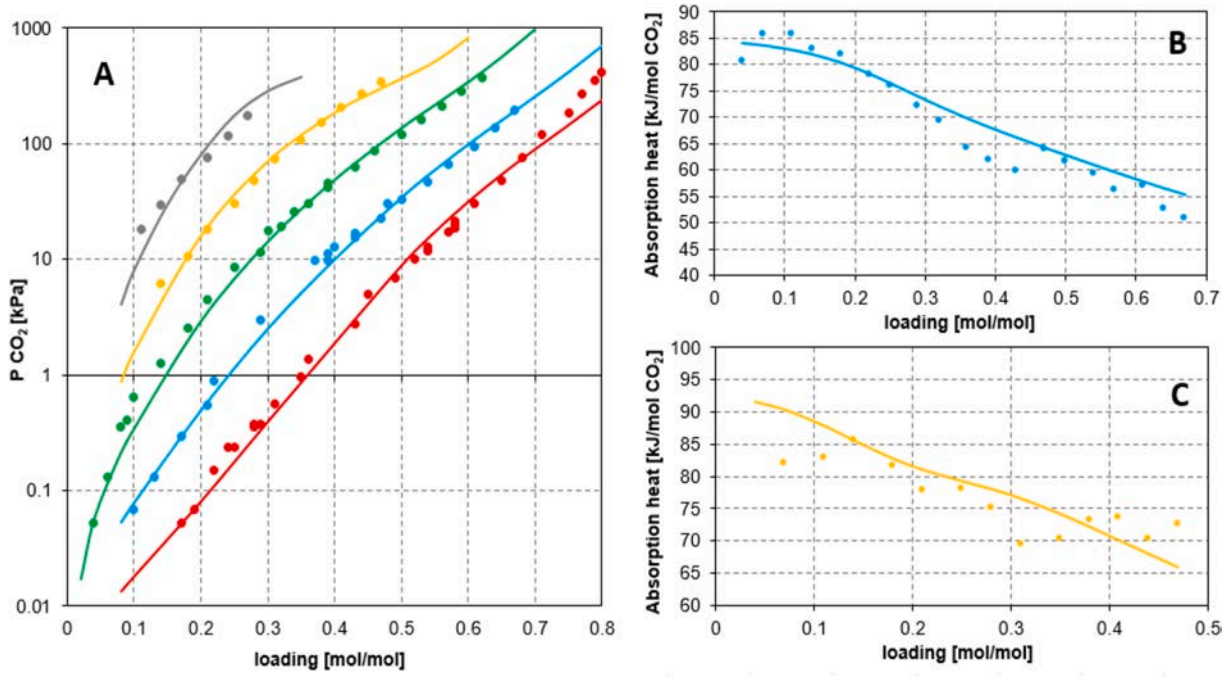

Fig. 1. Comparison between the Aspen Plus model predictions (solid lines) and the experimental data (dots) for (A) CO_2 partial pressure and (B, C) the heat of absorption of CO_2 at different temperatures: 40 °C (red), 60 °C (light blue), 80 °C (green), 100 °C (yellow), and 120 °C (grey). (For interpretation of the references to colour in this figure legend, the reader is referred to the Web version of this article.)

An Arrhenius-type kinetics has been considered for both reactions kinetics constants by assigning the activation energies (E_{act}) and exponential factors (A) determined from previous studies.

$$k_R = A \cdot \exp\left(-\frac{E_{act}}{RT}\right) \quad (5)$$

For AP, consistent kinetic models are available from two independent sources. Henny et al.'s (Henni et al., 2008) kinetics has been chosen since it is the most updated and it was obtained by direct measurements rather than using an indirect method as in Penny and Ritter (1983). Also for PRLD, the activation energies and exponential factors are taken from literature (Liu et al., 2017). Kinetic constants for inverse reactions are defined from the thermodynamic consistency using the corresponding equilibrium constants retrieved from the literature and reported in Gilardi et al. (2023)

In addition, kinetics is implemented also for reactions involving the bicarbonate formation from CO_2, in accordance with amine-based template models already available for similar blends in Aspen Plus® V11.0. The default kinetic by Pinsent et al. (1956), is used for these reactions (both direct and reverse).

$$CO_2 + OH^- \rightleftarrows HCO_3^- \quad (6)$$

Table 1
Reaction scheme for HS3 blend. Reactions are classified according to the type assigned in Aspen Plus.

Reaction	Reaction type	Source
$AP + H_2O + CO_2 \rightleftarrows APCOO^- + H_3O^+$	KINETIC	Reported in Table 2
$PRLD + H_2O + CO_2 \rightleftarrows PRLDH^+ + HCO_3^-$	KINETIC	
$CO_2 + OH^- \rightleftarrows HCO_3^-$	KINETIC	
$2H_2O \rightleftarrows H_3O^+ + OH^-$	EQUILIBRIUM	Available in Gilardi et al. (Gilardi et al., 2023)
$HCO_3^- + H_2O \rightleftarrows CO_3^{2-} + H_3O^+$	EQUILIBRIUM	
$APH^+ + H_2O \rightleftarrows AP + H_3O^+$	EQUILIBRIUM	
$PRLDH^+ + H_2O \rightleftarrows PRLD + H_3O^+$	EQUILIBRIUM	

Table 1 lists all the full reaction scheme for the HS3 blend. The proposed reaction scheme (used in the simulation environment) includes seven reactions: three of these are conventional reactions occurring in any amine system, and the remaining four are specific for the considered blend. Three reactions are characterized using an Arrhenius kinetic model (Table 2), thus, both direct and reverse reactions are defined taking advantage of the reaction rate as in equation (3). Four reactions are supposed to reach the thermodynamic equilibrium conditions as suggested in the literature for MEA in two different processes reported by Plaza (Plaza et al., 2009), Zhang (Zhang et al., 2009), and more recently by Rosha and Ibrahim (2023) for pre-combustion carbon capture and by Luo and Wang (2017) in an updated model for MEA using PC-SAFT. This default approach is proposed in available Aspen ELECNRTL framework and templates (Aspen Plus, 2019) as well also adopted in the literature for other conventional blends such as piperazine-activated MDEA (methyldiethanolamine, MDEA) (Mudhasakul et al., 2013), piperazine-promoted ammonia (Lu et al., 2017), and pure MDEA (Antonini et al., 2021). The same approach

Table 2
Reactions defined in kinetic mode for the HS3 blend.

Reaction	A	E/R [K]	Source	Notes
$AP + H_2O + CO_2 \rightarrow APCOO^- + H_3O^+$	$6.6 \cdot 10^{11}$	5454.8	Henni et al. (2008)	
$APCOO^- + H_3O^+ \rightarrow AP + H_2O + CO_2$	$2.22 \cdot 10^{12}$	6523.45		Calculated using thermodynamic consistency
$PRLD + H_2O + CO_2 \rightarrow PRLDH^+ + HCO_3^-$	$7.61 \cdot 10^{8}$	4924.0	Liu et al. (2017)	
$PRLDH^+ + HCO_3^- \rightarrow PRLD + H_2O + CO_2$	$4.79 \cdot 10^{11}$	8622.0		Calculated using thermodynamic consistency
$CO_2 + OH^- \rightarrow HCO_3^-$	$4.32 \cdot 10^{13}$	6667.84	Pinsent et al. (1956)	
$HCO_3^- \rightarrow CO_2 + OH^-$	$2.38 \cdot 10^{17}$	14,821.84		Calculated using thermodynamic consistency

is defined also for the model of the CESAR1 solvent (Morgan et al., 2022). The equilibrium constants are disclosed in our previous work on the thermodynamic modelling for the HS3 blend (Gilardi et al., 2023).

2.2.3. Mass transfer

Diffusion coefficients of the generic molecular species, i.e., CO_2, into the liquid mixture (D_i^L) is calculated by the software using the Wilke-Chang method (Poling et al., 2001). This model is based on equation (7), where the diffusion coefficient of a species in a liquid solution essentially depends on the boiling point molar volume of the generic species (V_{bi}), the temperature (T), the mixture composition (molar fraction *x*, molar mass *M* of the generic component *j*), an association factor (φ), and the viscosity of the liquid mixture (η^L). To characterize this last term, the Andrade mixing rule is implemented. Adaptive coefficients for this viscosity model are fitted to in-house and published amine-water mixtures viscosity data (Hartono and Knuutila, 2023). Details concerning the mixture viscosity model fitting using Andrade model can be found in Gilardi (Gilardi et al., 2023). The association factor φ is set to 2.26 for water and 1.0 for water, the default values by AspenTech.

$$\mathscr{D}_i^L = 1.17282 \cdot 10^{-16} \cdot \frac{\left(\frac{\sum_{j\neq i} x_j \cdot \varphi_j \cdot M_j}{\sum_{j\neq i} x_j}\right)^{0.5} \cdot T}{\eta^L \cdot \left(V_{b,i}\right)^{0.6}} \tag{7}$$

The effective diffusivity of an ion (*i*) in a liquid mixture with electrolytes has been evaluated using the Nernst-Hartley model (Horvath, 1985). This method is described by expression (8). In this equation, F is the Faraday's constant, z_i is the charge number of the specific ion under consideration, while l_1 and l_2 are parameters called IONMOB, specific to each single ion, to be assigned by the user. Due to the lack of specific data to properly tune the values of these parameters, the default value of 5.0 proposed by AspenTech has been set for all AP and PRLD ions as recommended in the user manual (Aspen Plus, 2019).

$$\mathscr{D}_i = \left(\frac{RT}{z_i F^2}\right) \cdot \left(l_{1,i} + l_{2,i} \cdot T\right) \cdot \sum\nolimits_k x_k \tag{8}$$

The binary diffusion coefficient of the ion with respect to a molecular species (D_{ik}) is set equal to the effective diffusivity of the ion in the liquid mixture (9):

$$\mathscr{D}_{ik} = \mathscr{D}_i \tag{9}$$

The binary diffusion coefficient of an ion *i* with respect to an ion *j* is set to the mean of the effective diffusivities of the two ions (10):

$$\mathscr{D}_{ij} = \frac{\mathscr{D}_i + \mathscr{D}_j}{2} \tag{10}$$

The Chapman-Enskog-Wilke-Lee method has been adopted to describe the diffusion coefficient of a gas molecule into a gas mixture (Poling et al., 2001). This is important to address the mass transfer limitations on the gas phase side. According to this method, the diffusion coefficient of a gas component in a low-pressure gas mixture is given in expression (11), where y stands for the molar fraction of the generic component in the gas mixture and D_{ij}^V is the binary diffusion coefficient in the gas phase. The latter can be calculated using expression (12), where M is the molar fraction, while σ and ζ are collisions and size parameters that are calculated by the simulator based on the polarity of the system (quantified by the dipole moment) and on the boiling temperature and boiling volume.

$$\mathscr{D}_i^V = \left(\sum\nolimits_{j\neq i} y_j\right) \cdot \left[\sum_{\substack{j=1 \\ j\neq i}}^{n} \frac{y_i}{\mathscr{D}_{ij}^V}\right]^{-1} \tag{11}$$

$$\mathscr{D}_{ij}^V = \left[2.1989 \cdot 10^{-22} - 5.0665 \cdot 10^{-23} \cdot \left[\frac{(M_i + M_j)}{M_i \cdot M_j}\right]^{0.5}\right] \cdot \frac{T^{1.5} \cdot \left[\frac{(M_i + M_j)}{M_i \cdot M_j}\right]^{0.5}}{\rho \cdot \sigma_{ij}^2 \cdot \xi_D} \tag{12}$$

The presented method for determining the diffusion of a component in a liquid and gas mixture has been exploited to build a mass transfer model for the absorber and for the stripper. The proposed rate-based model assumes an interfacial area of 0.82, in accordance with the MEA Aspen default model. The mass transfer and heat transfer correlation methods have also been taken from the reference MEA model: in particular, the Bravo-Rocha-Fair mass transfer correlation (BRF-85 in Apen Plus) is used for the mass transfer (Flagiello et al., 2021), while Chilton and Colburn analogy is used to calculate the heat transfer coefficients starting from the mass transfer coefficients (Tan et al., 2016). This is a common setup for absorber and desorber (Tan et al., 2016).

As a final remark, rate-based modelling is a general theory, well-established for modelling carbon capture processes (Neveux et al., 2013). Accordingly, mass transfer and kinetic limitations are considered in the simulation of the absorber and stripper to properly describe the CO_2 uptake and release, respectively (Gabrielsen et al., 2007). The framework is not solvent-dependent since it is general and it is extensively used in literature for pure amines and blends description (Antonini et al., 2021). The rate-based modelling is essential to properly describe carbon capture process especially for the absorption due to lower temperatures (Kvamsdal and Rochelle, 2008). In the simulation setup in Aspen Plus, it is crucial to define solvent properties such as density, viscosity, and diffusion coefficient because they influence the mass transfer which is one of the distinctive elements to classify and quantify the solvent performance (Razi et al., 2012).

3. Validation procedure and statistical analysis of the results

3.1. General description of the procedure

The full model (accounting for VLE, kinetics, and mass transfer) has been validated on pilot-scale data. To this aim, a simulation of the Tiller plant has been built in Aspen Plus to replicate the process layout and reproduce the experimental conditions during the pilot campaign.

54 different runs have been conducted at the Tiller plant for two CO_2 inlet gas concentrations representative of an NGCC flue gas (5.5 mol% on a dry basis) and a coal-fired power plant flue gas (11.8 mol% on a dry basis), respectively. The experimental campaign covered a wide range of lean loadings (0.03–0.15) and CO_2 capture rates (from 84% to 98%) to investigate the entire operating conditions domain for interest for large-scale carbon capture applications and to find the optimal operating conditions.

The model validation is split into two steps: first, the single units, i.e., absorber and stripper, have been validated separately in an open-loop configuration, and then, the full capture plant is simulated to test the performance of the combined system in a closed-loop layout. In the open-loop validation, the input to each column is assigned from the corresponding experimental observation/measurements, and the deviations for the outputs are expected to be "confined" to the tested unit, hence, there is no mutual influence and error propagation. In other words, a deviation in one of the outputs in the absorber (for instance, rich loading) does not influence the stripper validation because the two units are kept disconnected. The open loop flowsheets are depicted in Fig. 2A and B for the absorber and stripper, respectively.

The model has been finally tested on a close-loop system: the whole CO_2 capture process is simulated (Fig. 2C), thus the regenerated solvent obtained from the stripper is recycled back as input to the absorber. This last step is relevant to check the reliability and robustness of the proposed model and to verify that the interconnection between absorber and stripper is consistent; hence, the error propagation does not cause

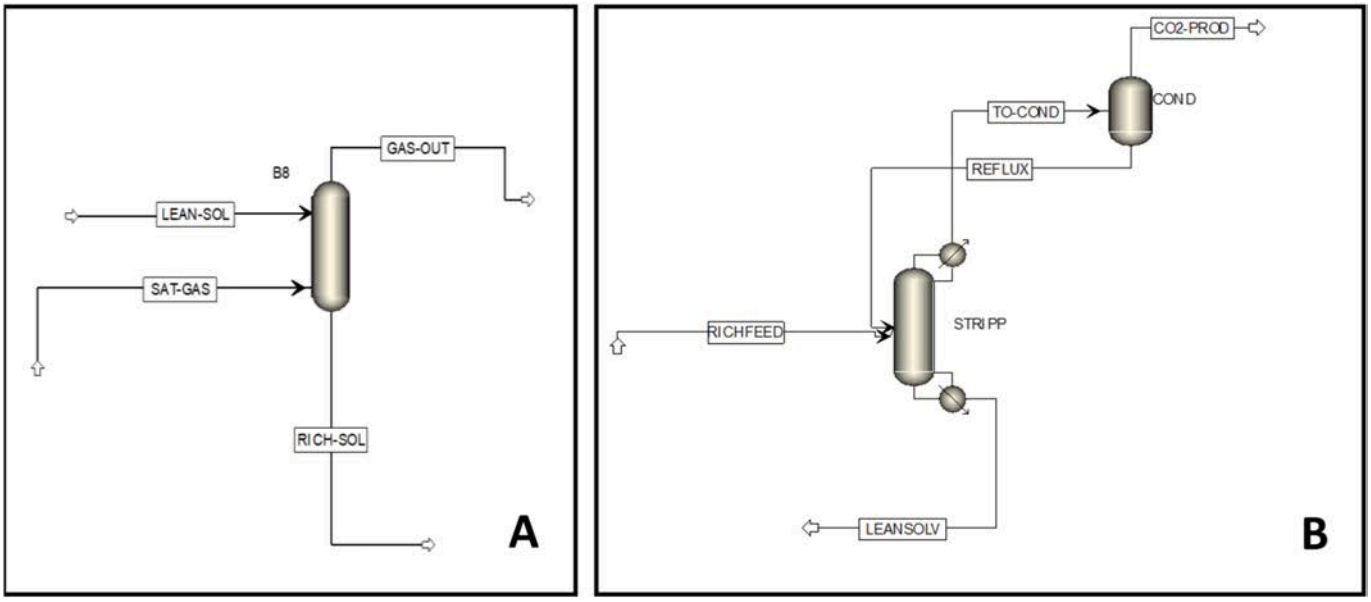

Fig. 2. Flowsheets developed in Aspen Plus V11.0 to reproduce the layout of the Tiller pilot plant: (A) absorber, (B) desorber for open-loop validation, and (C) full plant layout for close-loop validation.

larger deviations once the two subsystem interacts. To this aim, the duty, solvent, and gas inlet streams are fully defined by experimental observations, while the obtained percentage of captured CO_2 and the resulting lean and rich loadings are the compared outputs. 10 runs representative of the whole CO_2 content, loading and capture rate ranges of interest are considered for this additional validation. We focused on the runs which are most likely of interest for the industrial implementation of the HS3 solvent. Thus, we disregarded all the runs far from either optimal operative points or not feasible for an industrial case.

Table 3 gathers the inputs (assigned variables) and outcomes for both open- and closed-loop validation. The reported outcomes are the variables/outputs used to calculate the main process key performance indicators for assessing the model performance and reliability based on the discussed statistical analysis.

3.2. Statistical analysis

The accuracy and the prediction capacity of the model are verified by means of statistical analysis and indicators such as the Absolute Average Relative Deviation AARD%, as in equation (13), the Standard Deviation STD, defined in equation (14), the deviation (Dev), as in expression (15), and Average Relative Deviation (ARD%), defined in expression (16).

$$\mathrm{AARD\%} = \frac{1}{n} \cdot \sum_{i=1}^{n} \left| \frac{z_{i,exp} - z_{i,mod}}{z_{i,exp}} \right| \tag{13}$$

$$\mathrm{STD} = \sqrt{\sum_{i=1}^{n} \frac{\left(z_{i,exp} - z_{i,mod}\right)^2}{n}} \tag{14}$$

$$\mathrm{Dev} = z_{i,exp} - z_{i,mod} \tag{15}$$

$$\mathrm{ARD\%} = \frac{1}{n} \cdot \sum_{i=1}^{n} \frac{\mathrm{Dev}}{z_{i,exp}} \tag{16}$$

These indicators are relevant for the results post-analysis. AARD% and STD stand for the average relative and absolute deviations, respectively. The deviation (Dev) accounts for the gap between the model outcome and the corresponding experimental measurement. It stands for the direct assessment of the model against the experimental data. The Dev does not consider the absolute value of the deviation, and it is meant to graphically visualize if the model either over- or under-estimates a certain output variable in each single investigated run. The ARD% represents the average of all the deviations (Dev) for a certain variable. Positive values denote a model that tends to over-estimate a certain property, vice versa for a negative displacement. A good model should exhibit ARD% close to the null value meaning that the model is neither over- nor under-estimates a certain property (Buzzi-Ferraris and Manenti, 2011).

For the CO_2 absorbed/desorbed flows, four different experimental measurements are available from the pilot plant. CO2M1 refers to the CO_2 removed from the gas, i.e., the difference in the CO_2 mass flow at the inlet and outlet of the absorber on the gas side. CO2M2 and CO2M3 measure the amount of CO_2 either absorbed in or desorber from the liquid. Thus, they measure the difference between lean and rich loading in the absorber and in the stripper, respectively. CO2M4 is the measured CO_2 leaving the top of the stripper. For the absorber, CO2M1 and CO2M2 are totally equivalent indicators of the absorbed CO_2. Indeed, both are given as differences between two direct measurements on streams connected to the absorber. Thus, the open-loop validation of the absorber has been accomplished considering both datasets. Whereas, CO2M4 is likely the most reliable and affordable measurement among all the collected datasets because it is direct and not resulting from operations between two measurements which are potentially affected by their own experimental uncertainties. Measurements on the composition of the liquid phase are associated to slightly larger inaccuracies as experienced at the CO_2Lab in 100,000 h of different solvent testing. Therefore, we considered only CO2M4 for the open-loop validation of the stripper and for the close loop validation. In addition, the ARD% and AARD% of all the different experimental datasets are also calculated to define the experimental uncertainty on the collected CO_2 captured flow data measurements and to compare the order of magnitude of the uncertainty observed for the newly developed model prediction with the

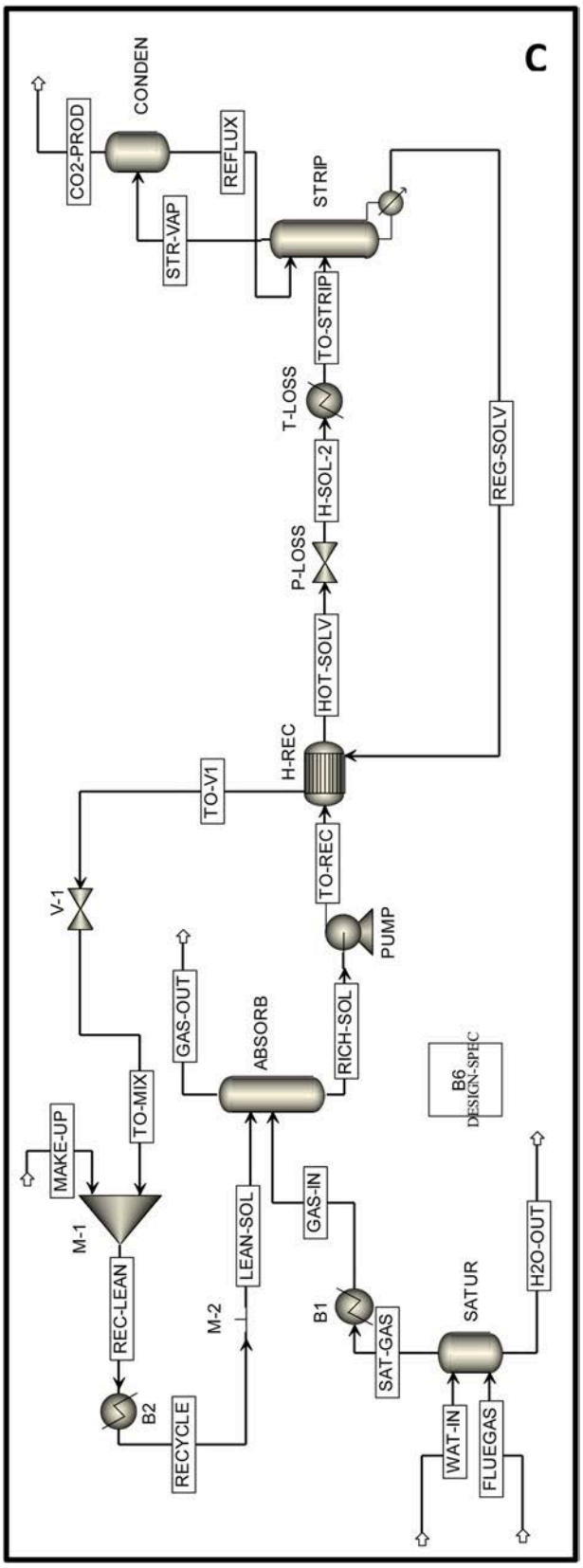

Fig. 2. (*continued*).

Table 3
Inputs and outputs for open- and close-loop validations. Streams refer to Fig. 2.

Unit	Inputs (assigned variables)	Outputs (compared variables), KPI
Absorber (open-loop) Fig. 2A	• LEAN-SOL (T, P, flow, and composition) • SAT-GAS (T, P, flow, and composition) • ABS diameter (D = 0.20 m) and packing height (H = 20 m) • Packing type	• Flow of captured CO_2 • RICH-SOL loading • Temperature profile in ABS
Stripper (open-loop) Fig. 2B	• RICHFEED (T, P, flow, and loading) • Reboiler duty • STRIP diameter (D = 0.15 m) and packing height (H = 15 m) • Stripper pressure • COND temperature • Packing type	• Flow of released CO_2 and specific reboiler duty (SRD) • LEANSOLV loading • Temperature profile in STRIP
Closed-loop Fig. 2C	• LEAN-SOL (T, P, flow) • GAS-IN (T, P, flow, and composition) • Columns layout (D and H) • Packing type • Stripper pressure • Reboiler duty	• Flow of captured CO_2 • specific reboiler duty (SRD) • lean (REG-SOLV) and rich (RICH-SOL) loadings (cycling capacity)

order of magnitude of the intrinsic experimental uncertainties. Experimental deviation is determined for measurements CO2M1, CO2M2, and CO2M3 assuming CO2M4 as a reference value. Remarkably, the mentioned experimental AARD% are all below 2.5%, which indicates the high quality of the collected data and the reliability of the adopted experimental apparatus. Moreover, the error in the material balance for the entire plant was below 1%.[3] This further confirms the accuracy of the experimental campaign carried out at Tiller. Tables (Table S1-Table S3) are available in the Supplementary Material with further quantitative details on experimental data uncertainties for all the CO_2 measurements distributed in the pilot plant. We preferred to perform two different statistical analyses accounting for the CO_2 concentration in the treated flue gas (5.5% and 12% on a dry basis) to distinguish the model performance when treating two different qualities of flue gas. The results of the statistical analysis are reported in the Results section (Section 5).

3.3. Simulation of the tiller pilot plant with the new Aspen Plus HS3 model

Simplified flowsheets for the Tiller pilot facility (Fig. 2) have been designed to reproduce the plant layout and the operating conditions adopted for each run during the experimental campaign. This preliminary step is required to test the developed Aspen model on Tiller plant data. Separated absorber and stripper simulations (Fig. 2A and B) are used for the open-loop validation. Conversely, the complete Tiller plant flowsheet (Fig. 2C) is exploited to test the close loop.

3.3.1. Absorber open-loop (Fig. 2A)

The absorber is a column packed with 20 m of Sulzer's Mellapak 2*X* packing. The Tiller pilot plant is also designed to shorten the packing, thus, the liquid solvent can be fed some meters below the top of the absorber column, as done for some of the runs to test the solvent performance at different packing lengths (i.e., shorter packed bed). The mentioned runs are 19, 20, and 21 (see Supplementary Material – Absorber temperature profile). This design solution allows to vary the height of the packing and test the solvent for a different absorber configuration. The pressure drop inside the column is assigned based on the outcomes of the pilot plant campaign. The results of the pressure drop are comparable to those estimated using internal subroutines implemented in Aspen Plus for the calculations of pressure drop in structured packings. The gas (GAS-IN) and the solvent (LEAN-SOL) inlet streams are fully characterized in terms of temperature, pressure, mass flow rate and composition to coherently replicate the corresponding experimental inputs.

3.3.2. Stripper/desorber open-loop (Fig. 2B)

For the stripper (STRIPP), the feed (RICHFEED in Fig. 2B) is defined by providing temperature and pressure values as in the pilot plant campaign. Due to the lack of specific data collected for the input to the desorber, the mass flow and the composition of stream TO-STRIP are instead assumed equal to the ones measured for the RICH-SOL stream (solvent exiting the absorber). This assumption is reasonable considering that there is no stream splitting between the absorber. Moreover, the Aspen ELECNRTL model can calculate directly the actual solvent speciation of RICH-FEED (in Fig. 2B) based on the temperature and pressure at the inlet of the desorber and apparent composition from the RICH-SOL stream (in Fig. 2A). Indeed, for what concerns the flow composition, it is reasonable to assume that the apparent composition in CO_2, H_2O, and amines (i.e., the relative quantities of the components by neglecting the speciation) is unchanged owing to negligible water losses between the bottom of the absorber and the top of the stripper. The apparent composition indicates the system composition obtained by neglecting the system speciation. In other words, the temperature changes from the bottom of the absorber to the top of the stripper. This influences the speciation of the solvent (i.e., the quantity of each ions), but not the loading based on apparent composition (i.e., the amount of CO_2 confined into the amines) because the material balance must be satisfied.

3.3.3. Close-loop flowsheet (Fig. 2C)

In the full plant flowsheet, the flue gas (assigned dry volume composition) is conveyed to a saturator. Since saturation temperature and pressure are known from the experimental campaigns, the saturator is modelled as a flash at an assigned temperature and pressure. A chiller (B1) adjusts the temperature of the flue gas. This device, which is present at Tiller facility, tunes the flue gas to the desired temperature. A design-spec tool is added in the flowsheet to modify the mass flow of the FLUEGAS stream so that the gas flow entering the absorber (stream GAS-IN) is equal to the corresponding experimental data. Temperature, pressure, flow rate, and mass composition are assigned for the LEAN-SOL stream. For the absorber (ABS), pressure and pressure drops are assigned too. The solvent enriched in CO_2 (RICH-SOL) is pumped to a higher pressure with respect to the top stage of the stripper, to account for the overall pressure drops and the static pressure for pushing the solvent from the ground to the top stage of the column. The discharge pressure from the rich pump is such that, on average, the corresponding solvent pressure downstream H-REC is around 3 bar. A heat recovery occurs between the rich solvent to be fed to the stripper and the lean solvent recovered from the bottom of the stripper itself. The outlet temperatures of both cold and hot side streams are available from the pilot plant. For the sake of process simulation, the hot outlet-cold inlet approach temperature is imposed as a specification, and its value is assigned directly from the experimental observations. For simplicity, a valve at assigned outlet pressure (P-LOSS) and a heat exchanger at assigned outlet temperature (T-LOSS) are modelled to account for the pressure and temperature losses experienced in the pilot plant in the section from the heat recovery (H-REC) to the inlet of the desorber, respectively. The desorber (STRIPP) is simulated as a rate-based rad-frac module with 15 m of packing (Sulzer Mellapak 2*X*). The top condenser

[3] Results and data from the experimental campaign at Tiller will be public at the official webpage after the approval form the EU Commision Officer (Deliverable D2.4 – *HS-3 Campaign at Tiller plant*).Link - https://cordis.europa.eu/project/id/884266/results.

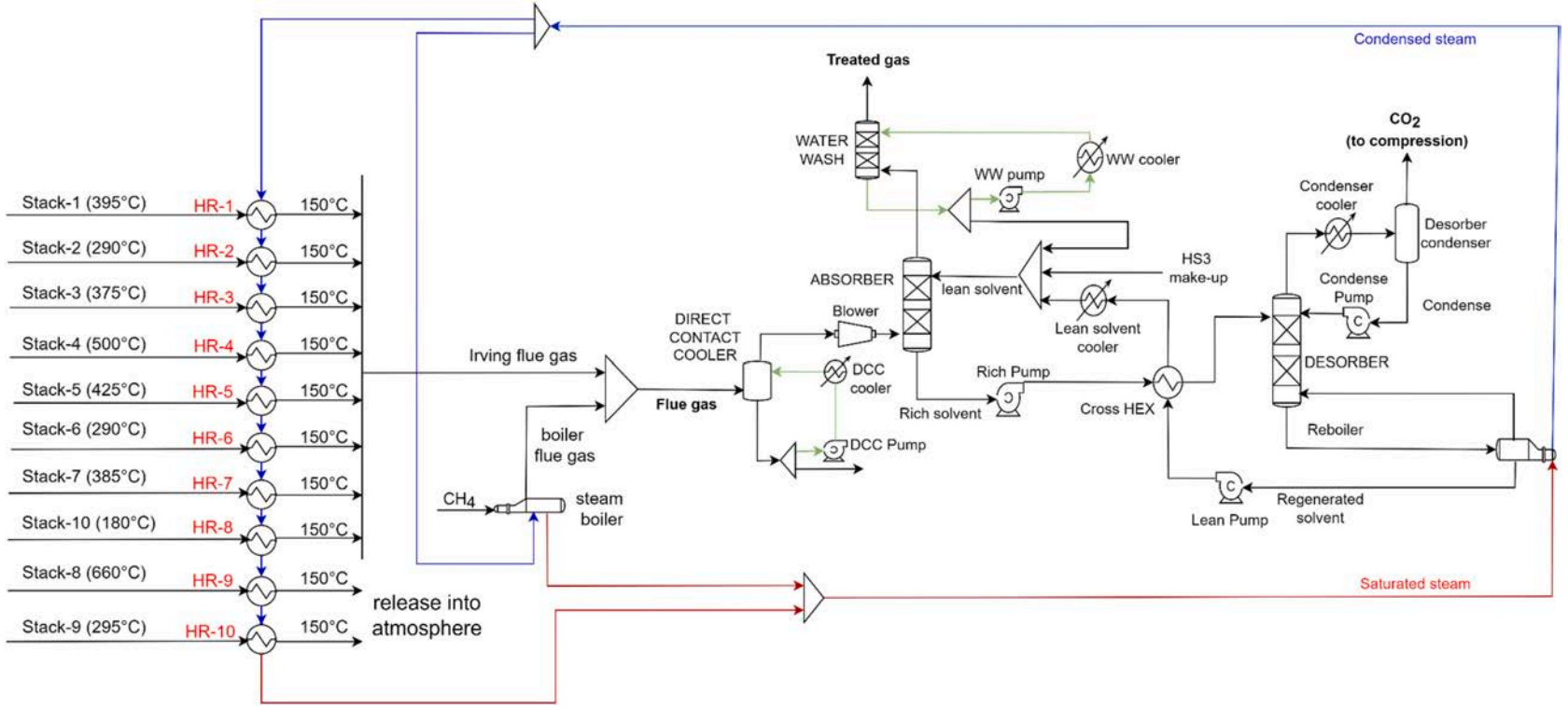

Fig. 3. Schematic flowsheet of the plant designed for CO_2 capture from the Irving Whitegate Oil refinery.

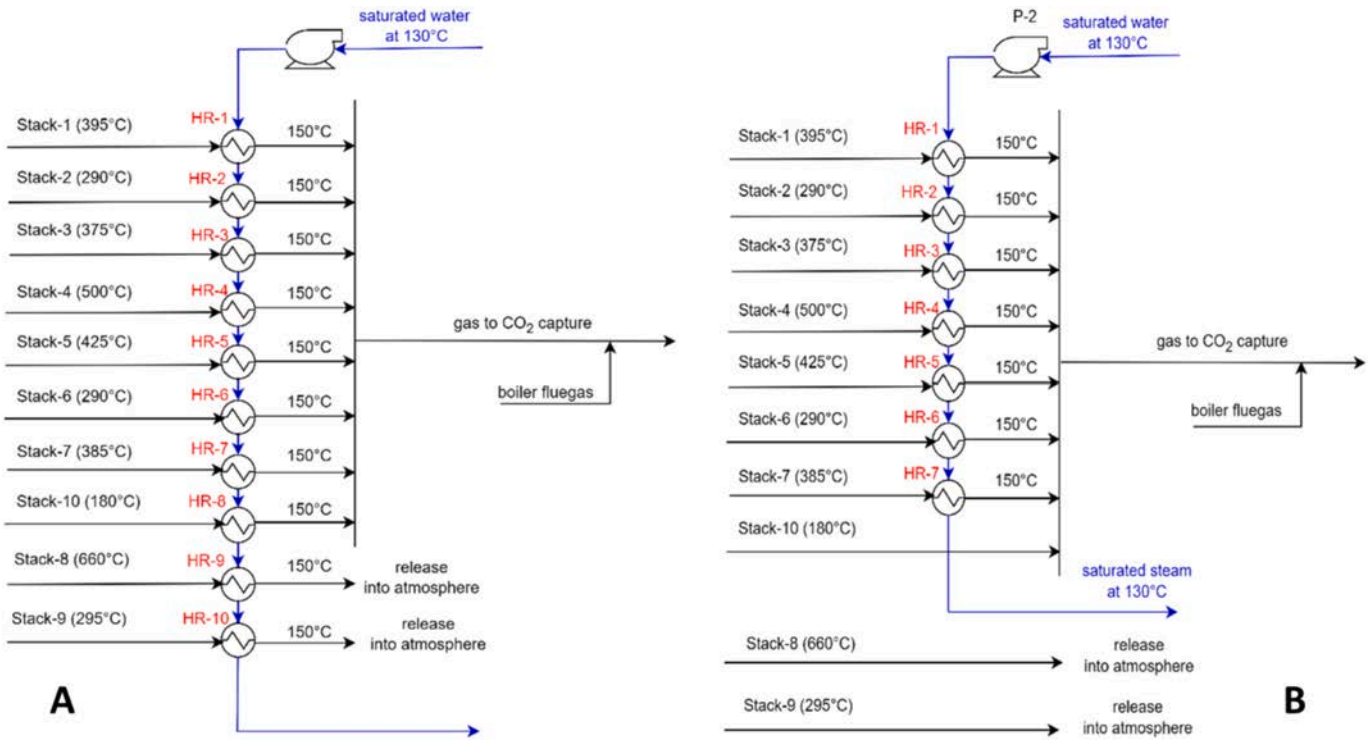

Fig. 4. Preliminary design of the heat exchanger network for the thermal energy recovery from the flue gas: (A) heat recovery from each stack and (B) heat recovery from seven streams.

(CONDEN) is modelled as a separate flash at assigned temperature and pressure. The recovered solvent is recycled back to the absorber after heat recovery, expansion back to the absorber pressure in V-1 and mixing with a make-up water stream accounting for water losses within the plant. The mixed solvent is cooled in a chiller (B2) to the same temperature of the LEAN-SOL stream before being recycled back to the absorber. Further details on the Tiller CO_2 laboratory plant layout and operation mode are available elsewere (see footnote 3).

4. Industrial case application: the Irving Whitegate Oil Refinery (Ireland)

4.1. Design of a CO_2 capture plant for the treatment of the irving oil refinery flue gas

The validated model is used for the assessment of a real industrial case study. Eight stacks from the Irving Whitegate Oil refinery flue gas are conveyed to the CO_2 capture plant. The overall CO_2 concentration obtained by summing the considered stacks is 7.65 mol% on a wet basis. A schematic representation of the base process flowsheet designed for this application is drawn in Fig. 3. The same flowsheet is adopted both for the HS3 and the MEA-based process, to guarantee consistency for the comparison between the two solvents. In other words, the number and type of unit operation are unchanged. The next paragraphs define the assumptions and rationale behind the adopted assumptions to build the flowsheet for the case study.

4.1.1. Stacks definition and pretreatment

The stacks (available at high temperatures ranging from 250 °C to 600 °C) are cooled down to 150 °C in a train of process-process heat exchangers (HR-1 to HR-10). The stacks mass flow, pressure, and CO_2 content are confidential. The gas-side outlet temperature is set to avoid any condensation of acid gas, i.e., NO_x, which occurs below 150 °C (Fostås et al., 2011). This event leads to unacceptable generalized corrosion of the pipelines and units (Szulc et al., 2018). Noteworthy, a temperature of 150 °C on the saturated water/steam side allows keeping a minimum temperature difference of 20 °C across the gas-transition phase liquid heat exchanger. The steam temperature (e.g., 130 °C) is a common choice in carbon capture plants since the desorber works in the pressure range of 1.8–2.1 bar ab To achieve an effective solvent regeneration (Oexmann et al., 2012) while avoiding large thermal degradation (Vevelstad et al., 2023). This is part of the general know-how for carbon capture plants and understanding of the HS3 solvent properties, acquired within the REALISE CCUS project. Some more details on the criteria adopted for this preliminary heat integration are presented in the following subsection. The control of the outlet temperature of the flue gas could be an issue for the energy recovery system. However, Figs. 3 and 4 are simplified schemes to depict how it is possible to recover enthalpy from hot flue gas from the stacks. Any considerations about the process controllability and detailed design of the section are not relevant to the present work since our assessment relies on global energy and material balances. Stacks 8 and 9 are not conveyed to the carbon capture due to the limited mass flow and little CO_2 content (i.e. <1% vol) which make streams not suitable for capture in an industrial application (Bains et al., 2017). These are directly released to the atmosphere after heat recovery. Noteworthy, stacks 8 and 9 contributes to only 1.3% of the total CO_2 emissions of the site. Solvent-based capture is energy-intensive as the CO_2 concentration drops. In this way, we avoided the dilution of the CO_2 in the fed flue gas. For instance, in the industrial practice, the flue gas leaving aluminum factory contains 1% vol. CO_2, but there are strategies to increases its concentration at least around 3–4% volume and make the carbon capture suitable (Berstad et al., 2013). This justifies our assumptions to neglect stacks 8 and 9.

4.1.2. Carbon capture: process description and assumptions

4.1.2.1. Direct Contact Cooler (DCC). The precooled flue gas is further cooled down in a Direct Contact Cooler (DCC). Since the cooling water circuit is assumed to provide Cooling Water (CW) at an inlet temperature of 20 °C, the process water flow circulating inside the DCC loop can

be available at 25 °C. This assumption on cooling water temperature is based on a previous study reporting cooling water temperature in Dublin (Ireland) throughout the year (Costelloe and Finn, 2003), which ranges from 8 °C in January (best condition) to 20 °C in July (worst scenario). For the sake of conservativeness, the cooling water temperature is set to 20 °C. Furthermore, a 3 °C temperature approach is considered for the DCC, so that the flue gas leaves the top of the DCC at 28 °C. It is important to maintain the temperature of the flue gas leaving the DCC as low as possible to achieve a temperature for the gas entering the absorber below 60 °C, i.e., the lowest as possible (Arias et al., 2016), otherwise the absorber efficiency drops due to large water evaporation and lower solubility of the CO_2 in the solvent (Putta et al., 2017). Gao and Rochelle observed that the control of the temperature of the flue gas and within the column is crucial to preserve the absorber performance (Gao and Rochelle, 2020). Indeed, the flue gas temperature rises considerably in between the DCC and the absorber due to compression. The column is simulated using a rate-based approach; the Sulzer Mellapak 250*X* packing height is set to 3 m, while the diameter is calculated so that the unit works at 70% of the flooding velocity (Tsay et al., 2019). This higher margin with respect to the default 80% flooding velocity criterion proposed as default by Aspen Tech (Aspen Plus, 2019) allows to reduce the pressure drops inside the column while having a larger exposed surface to contact the liquid and gas phase. Chao et al. experimentally showed that 65–70% is the optimal flooding for Mellapak 250*X* to minimize the operating costs (Wang et al., 2015). Part of the water present in the flue gas condenses inside the DCC, reaching saturation conditions at the top stage. For this reason, the cooling water loop circulating in the DCC is provided with a splitter to discharge this excess water content. The condensed water in excess must be sent to water treatment since it contains CO_2 and other acid gases.

4.1.2.2. Blower. A fan (C-1) allows overcoming the total pressure drops occurring inside the preliminary heat recovery heat exchangers (HR-1 to HR-10), inside the DCC, the absorber (ABS) and the water wash (WW). The pressure drop associated with the structured packing only has been doubled to account for other sources of concentrated pressure drops such as liquid and gas distributors, demister, headers, and so forth (Zhang and Lu, 2015). The pressure drop impacts the electricity consumption because the blower is expected to compensate for the pressure drop of the gas. Moreover, the higher the pressure drop, the higher the outlet temperature of the flue gas from the fan owing to the gas compressibility. This is reflected in higher water evaporation at the bottom of the absorber (Putta et al., 2017). To compensate for the water loss, either more cooling water is fed in the water wash or more water make-up should be accounted for to re-establish the water balance within the system. The effect on the cooling water is not substantial when DCC, i.e., pre-cooling, is effective as in the proposed case study, e.g., cooling water at around 20 °C, i.e., worst case, (Hetland et al., 2009). The fan is modelled assuming an isentropic efficiency of 80%. The total pressure drop to be overcome is also a function of the total absorber packing height, but it is in any case included between 0.2 and 0.23 bar for both solvents (i.e, HS3 and MEA). As clarified also later in Section 4.2, the heat recovery units have been optimally designed by means of Aspen EDR (Exchanger Design and Rating), considering flat plate heat exchangers type in counter-current configuration. The sizing is important to estimate the flue-gas side pressure drops, which are close to 0.09 bar with minimal variations among the different units. This value is adopted as input for the design of the fan in the CO_2 capture plant.

4.1.2.3. Absorber (ABS) and water wash (WW). CO_2 is removed inside an absorber (ABS), which is packed with Sulzer Mellapak 250*X*. The solvent flow to be fed to ABS is determined to ensure 90% capture ratio of the total entering CO_2. The interactive sizing tool available in Aspen Plus V11 has been exploited to estimate the design diameter for the absorber and the stripper. 70% flooding velocity has been adopted as the design basis, based on prior literature for Mellapak 250*X* in carbon capture (C. Wang et al., 2015).

The treated gas is conveyed to a water wash (WW) to lower the residual amine content in the gas to less than 5 ppm. This threshold is chosen on the basis of current legislations on amine emission tolerance. For example, 6 ppmv is the maximum daily average total amine concentration limit according to the Norwegian environmental authority (Shah et al., 2018) released from middle-scale demonstration plant. For larger-scale demonstrative plants, there are more flexibible limits, such as ROAD permit (2012). The ROAD allows amine emissions up to 23 mg/Nm^3 as recommended in the Scottish Environmental Protection Agency report on amine emissions from carbon capture plants (SEPA, 2015).

The diameter of the water wash is set equal to the absorber's one. This is a technical constrain, indeed, the water wash column is conventionally stacked just above the absorber and it is better to have similar cross sections. The water-wash packing height is selected as the minimum height required to reach the specification of the residual amine content in the treated gas using a circulating water rate to get maximum 70% flooding inside the washing section. The washing water circulates in a closed loop to avoid continuous integration of large amounts of fresh water into the plant. This loop includes a water circulation pump and cooling water is the coolant to re-establish the temperature of the recycle. The pressure drop inside cooling water loops is set to 2 bar for the sake of pump costs estimation. This value account for the static head pressure. A makeup freshwater stream is also included to close the water balance of the plant.

The rich solvent is pumped in P-1 to a pressure that must be sufficient to reach the stripper operating pressure and to overcome at the same time the pressure drops in the lean-rich heat recovery exchanger (HR-11) and the pressure drops required to feed the solvent to the stripper at its upper stage. To this purpose, the pressure drop in HR-11 is set to 0.35 bar in accordance with the rules of thumb proposed by Seider et al. (2017), while gain a pressure drop of 1 bar per 10 m of vertical elevation is assumed for accounting for the static pressure. A temperature approach of 10 °C is imposed to HR-11.

4.1.2.4. Stripper/desorber (DES) section. The rich solvent is then sent to the desorber (DES). The desorber column has a top condenser working at a temperature of 30 °C, where CO_2 is recovered from the top, while lean solvent is withdrawn from the bottom and redirected towards the absorber after heat integration in HR-11 with the rich solvent to be regenerated. The stripper is modelled as a rate-based unit, but kinetics is disregarded since it is based on experimental data collected at much lower temperatures (25–40 °C) with respect to the ones observed inside this column. This assumption is often adopted since desorption reactions are fast enough so that mass transfer becomes the limiting step as noticed with two different solvents, namely MEA and piperazine, on a pilot scale by Li et al. (2016) and Van Wagener and Rochelle (Van Wagener and Rochelle, 2011), respectively. The negligible effect of the kinetics on the desorber performance has been addressed in an in-silico assessment by Madeddu et al. by considering several possible operating conditions (Madeddu et al., 2018). The lean loading of the hot lean solvent leaving the reboiler is set equal to the lean loading of the solvent fed to the absorber. This specification allows closing the CO_2 mass balance and it considerably speeds up the convergence of the unit with respect to alternative specifications such as the bottom temperature. The proposed system represents a real plant, including pilot facilities. Indeed, in a real capture plant, the liquid circulation rate is assigned, whereas the duty for the solvent regeneration is the manipulated variable. Finally, the heat loss in large-scale facilities is neglected owing to lower exposed external surface/volume ratio as Lawal et al. assumed in modelling and then demonstrated in a large carbon capture plant (Lawal et al., 2012).

The regenerated solvent is pumped to guarantee sufficient pressure

to reach the top of the absorber, and it is further cooled in a chiller and recycled back to the absorber. Heat exchangers, i.e., lean solvent chiller, the top condenser cooler (stripper), the DCC cooler, and WW cooler, have been modelled as coolers; the cooling water utility enters at 20 °C and is discharged at 35 °C. In addition, a recirculation pump for water circulation inside the DCC and WW loops is included.

Since the amount of heat recovered in HR-1 to HR-10 is not enough to provide the entire reboiler duty, a steam boiler is installed. The stacks from the refinery are collected with the flue gas generated in the steam boiler. The steam boiler is designed to cover the thermal duty for the CO_2 capture plant not recoverable from the stacks. The amount of methane (assumed pure) to be burnt in the steam boiler to generate the requested duty for the solvent regeneration is calculated from expression (17), where LHV stands for the lower heating value of methane (50 MJ/kg) and η is the efficiency of the boiler, assumed 0.8 (Pellegrini et al., 2015). Methane is supposed to be fully converted into carbon dioxide and steam. A standard 15 % molar excess air is considered for the calculation of the generated flue gas composition (Schiffhauer and Veitch, 2009).

$$F_{CH_4} = \frac{Q}{LHV_{CH_4} \cdot \eta} \tag{17}$$

The molar flowrate of the flue gas from the steam boiler is calculated according to expression (18), where MW is the molecular weight of methane, Q_{reb} is the total regeneration column's reboiler duty and $Q_{rec.\ stacks}$ is the amount of heat recovered by cooling each refinery stack down to 150 °C in the abovementioned heat recovery section. The flue gas leaving the steam boiler is also conveyed to the absorber.

$$F_{boiler,flue\ gas} = \frac{Q_{reb} - Q_{rec-stacks}}{LHV_{CH_4} \cdot \eta \cdot MW_{CH_4}} \tag{18}$$

4.2. Preliminary design of heat recovery system: hot flue gas – steam generation thermal coupling

Saturated steam at 130 °C is the hot utility for the solvent regeneration. The assigned saturation temperature guarantees a minimum approach temperature of 10 °C accross the reboiler, being the temperature at the bottom of the stripper close to 120 °C. The steam condenses inside the reboiler and is recovered in the form of saturated water. Thus, it has to be re-vaporized prior to recirculation to the reboiler. The steam generation via condensed water re-vaporization is an energy-intensive process. Minimizing this heat duty is crucial for the economic sustainability of the proposed plant. To this purpose, a network of recovery heat exchangers distributed in a parallel configuration where each single refinery stack gets cooled down by exchanging heat with the utility used in the CO_2 capture process for solvent regeneration has been designed. Indeed, the Irving oil refinery flue gas stacks are available at temperatures ranging from 180 to 660 °C, as shown in the data sketched in Fig. 4. Since the absorber operates at much lower temperatures (40–50 °C), the residual heat could be exploited for some energy integrations within the capture plant to reduce to the lowest extent the need for external steam to meet the carbon capture plant energy requirements. As it will be clear in the result section, a substantial fraction of the energy demand for the regeneration is supplied as saturated steam recovered from the energy integration system, where the enthalpic excess of the hot refinery stacks is recovered and exploited as heat source. The flue gas outlet temperature is set to 150 °C to keep a 20 °C approach temperature between the process fluid and the utility side. As already discussed, the outlet temperature of the flue gas leaving the heat exchanger network is set to 150 °C to avoid any condensation of acids before entering the DCC column (Shatskikh et al., 2017). The control of the outlet temperature of the flue gas could be an issue for the energy recovery system. Fig. 4 report simplified schemes without any purpose for a detail engineering.

Since the ten stacks from Irving Whitegate Oil have different flow rates and temperatures, for some of them, the heat recovery is much more effective than others. Moreover, the purchase of ten process-process heat exchangers in the carbon capture plant flowsheet, as depicted in Fig. 4A, can significantly impact the investment costs, meaning that a trade-off between the number of heat exchangers and the total amount of heat recovered should be found for a smart plant design. For instance, Fig. 4B reports an alternative layout where only seven out of the ten stacks have been considered for energy recovery. A comparative preliminary cost assessment referred to the same case study (Gilardi et al., 2022) showed that considering all ten heat recoveries allows to minimize the total costs of the capture plant when reference MEA solvent is adopted. Therefore, the layout depicted in Fig. 4A is also proposed for the case study of the Irving Oil Refinery with HS3.

First, the heat exchangers network has been modelled to quantify the total duty recovered from the refinery stacks and the corresponding impact in terms of reduction of the overall energy requirements of the CO_2 capture process. In the second step, each heat exchanger has been optimally designed by means of Aspen EDR (Exchanger Design and Rating), considering flat plate heat exchangers type in counter-current configuration. This sizing is important to estimate the flue-gas side pressure drops, which are close to 0.09 bar with minimal variations among the different units. The pressure drop has been considered for the design of the fan.

4.3. Sensitivity analysis for the case study optimization

The optimal operating conditions for the CO_2 capture plant described in Section 4.1 have been determined by means of a sensitivity analysis both for MEA and for HS3 solvents. A baseline case is defined as follows. The inlet solvent temperature is set to 43 °C; a CO_2 capture rate of 90% is assumed, and the stripper pressure is set to 1.8 bar. For MEA solvent, the minimum absorber and stripper packing heights are set to 6 m and 8 m, respectively, based on the results of a previous CO_2 capture plant optimization work for a similar flue gas composition (Ghilardi, 2020). For HS3, 16 m is set as a conservative starting absorber and stripper packing height, since experimental pilot scale campaigns have pointed out that, under comparable operating conditions and desired capture performances, HS3 solvent kinetic is slower. The baseline simulation considers the top stage for the rich solvent feeding to the stripper column. Finally, the lean loading is set to 0.27 for MEA, based on a previous optimization work with the same default MEA Aspen framework by Ghilardi et al. (Ghilardi, 2020). The lean loading is 0.07 for HS3, corresponding to the optimal loading found during the experimental campaign at Tiller. No water wash is considered for the baseline process, since it has no impact on the energy requirements, thus on the SRD which is the parameter to be minimized.

The aim of the sensitivity analysis is to minimize the specific reboiler duty (SRD), which is a key performance indicator of the energy requirement. The SRD is defined as the thermal duty demand per unit of captured CO_2 ($MJ_{th}/kg_{CO2\ capt}$). Starting from the proposed baseline simulation, the following parameters are optimized in line with the methodology proposed by Abu Zahra et al. (Abu-Zahra et al., 2007b).

- lean loading (α): the trend of the SRD as a function of α is monitored in a range between 0.18 and 0.36 for MEA and between 0.05 and 0.12 for HS3. For the MEA, we based on Abu Zahra et al. (Abu-Zahra et al., 2007b), while, for HS3, we focused on the loading domain where the Tiller campaign found the optimum for 90% capture ratio with the tested flue gas compositions.
- desorber pressure: a range between 1.5 bar and 2.2 bar with a step of 0.1 bar step (Abu-Zahra et al., 2007a). At increasing pressure, the SRD lowers, but the temperature at the bottom of the column increases. The optimal pressure is constrained to the quality of the steam available for the regeneration (Kvamsdal et al., 2016) and the reboiler temperature does not overcome 122 °C. This condition is important to maintain a sufficient approach temperature with

respect to the hot utility side, i.e., saturated steam at 130 °C (Oexmann et al., 2012).

- Lean solvent temperature: a reduction in the solvent temperature does not modify appreciably the SRD (Adu et al., 2020). On the one hand, a higher solvent temperature allows for reducing the cooling water consumption in the chiller, while amine and water losses inside the absorber increase. 43 °C is therefore selected for both solvents as a trade-off between these two opposite trends (see Section 5.2.2 for details).

In addition, the packing height for absorber and stripper can be optimized.

- absorber packing height: the SRD profile for several loadings (α) is investigated at different packing heights, with a discretization step of 2 m. The optimal height is selected as the minimum height for which an increment in the SRD lower than 1% is observed with respect to the previous case study;
- stripper feed stage: selected as the one for which the SRD is minimized;
- desorber packing height: SRD has been calculated at different heights, with a discretization step of 2 m. The optimal height is selected according to the same criteria adopted for the absorber;

Considering the lack of a standardized procedure for this kind of optimization, a threshold of 1% decrease is considered to stop the analysis.

A summary of the variables included in the process optimization, the tested ranges, and the rationale for exploring their effect on the performances of the carbon capture plant are gathered in Table S4 in the Supplementary Material.

5. Results and discussion

5.1. Aspen Plus HS3 model validation

The full model (including thermodynamics, kinetics, and mass transfer) has been tested on pilot-scale data following the procedure described in Section 3.

5.1.1. Open-loop validation for the absorber

The plots of the residuals show the relative deviations (dots) between model predictions and pilot-scale Tiller data for the captured CO_2 mass flow and the rich loading are reported in Fig. 5. Table 4 gathers the AARD% and ARD% for all the investigated KPIs (see Table 3) associated with the absorber: the statistical analysis is available both including all runs, and by differentiating the datasets according to the CO_2 inlet content for 5.5 vol% and 12 vol% CO_2 initial flue gas concentration, respectively. Table S5 and Table S6 gather the absolute and relative deviations for the main KPIs in the validation of the open-loop for the absorber.

5.1.2. Open-loop validation for the desorber

Fig. 6 shows the results of open-loop validation for the stripper: the compared outputs are the CO_2 flow recovered from the top of the stripper as well as the lean loading of the regenerated solvent. In compliance with the procedure adopted for the absorber, the statistical analysis for the desorber validation is available both including all datasets together and differentiating the datasets according to the CO_2 inlet content for 5.5 vol% and 12 vol% CO_2 initial flue gas concentration, respectively. Numerical results are gathered in Table 5. More details on the relative and absolute errors for the validation of the stripper open-loop are gathered in Table S7 and Table S8 in the Supplementary Material.

5.1.3. Statistical analysis of the open-loop validation

Looking at the outcomes of the statistical analysis including all datasets, it is remarkable that the maximum observed AARD% is in the order of 5%. More specifically, for 80% of the runs the relative deviation on captured CO_2 flow is lower than 5%, while for almost 91% of the runs it is below 10%. A slightly higher discrepancy is observed for the desorbed CO_2 flow: 67% and 89% of the runs exhibit a relative deviation below 5% and 10%, respectively. The only exception is the lean loading; however, the higher discrepancies observed for this indicator are caused by the very low numerical values of the lean loadings. Indeed, 72.7% of the runs show a deviation lower than 20%, which corresponds on average to an absolute error of 0.015 mol/mol. The STD for lean loading is close to 0.01 mol/mol. A few examples of temperature profiles comparing the model prediction and the experimentally observed profiles inside the absorber and the stripper are available in Fig. 7. The selected case studies are representative of both initial CO_2 concentrations and characterized by different lean loadings and capture rates. It is worth mentioning that the bottom, the top, and the peak/bulge temperatures have a significant impact on the carbon capture process (Kvamsdal and Rochelle, 2008). The bottom temperature influences the heat recovery in the cross heat exchanger in Fig. 4, in turn, the reboiler duty. The top stage temperature affects the water wash design and the peak temperature impacts the CO_2 absorption kinetics. All these three temperatures are predicted with sufficient accuracy in most of the investigated runs. For the stripper, the most relevant measurement is the reboiler temperature, which is directly related to the energy for the solvent regeneration. A full comparison between the temperature profiles resulting from all the tested runs and the corresponding experimental data for both the absorber and the stripper are provided in the Supplementary Material.

Noteworthy, the AARD% does not overcome 7% regardless of the CO_2 content in the flue gas for all the KPIs for the absorber and stripper. Such deviations from the model can be considered acceptable for process design and scale-up purposes. As mentioned, there are four different CO_2 measurements installed in the Tiller pilot plant (Section 3.2). The corresponding uncertainty of the experimental datasets used for comparison is around 1.5%–2% as reported in the Supplementary Material (Table S1-Table S3).

It is evident that the model predictions for the capture rate estimate are more accurate for the runs with flue gas at 5.5 vol% CO_2. Indeed, for 12 vol% CO_2 flue gas, the STD for the model prediction increases by a factor of 2.06 and the AARD% increases by 54%. Consistently, similar considerations hold for the prediction accuracy of the CO_2 flow released in the desorber, being the AARD% calculated for the 12 vol% dataset 2.75 times the AARD% for the 5.5 vol% dataset.

However, it is remarkable that for the runs carried out with 12 vol% also the intrinsic experimental data uncertainty is much higher (Table S2 and Table S3). Indeed, the Tiller data collected at 12% vol. Of CO_2 present a STD which is double if compared to the same runs with 5% CO_2 content. The same increment in the uncertainty is observed for the model predictions and the corresponding AARD increases by 37% on average if compared to the dataset at 5.5 vol% CO_2. This observation can at least partially justify the higher deviations observed in the developed Aspen model flue gas at 12% vol. Of CO_2.

Conversely, the temperature profiles inside the absorber are more accurate for the runs with 12 vol% CO2 (AARD <3%), while the dataset describing runs at 5.5 vol% shows AARD% over 6%, corresponding to a standard deviation close to 4 °C. The reason for the higher discrepancy is given by the tendency of the model to overestimate the temperature in several runs in the portion of the plot between the peak temperature and the bottom of the column (see Supplementary Material). The discrepancy between the model accuracy at lower and higher flue gas CO_2 concentration is much less evident for the desorber temperature profiles, where a comparable AARD% and STD are obtained for both datasets at 5.5% and 12% vol. Of CO_2. For the sake of completeness we added tables (from Table S4 to Table S8) in the Supplementary Material. These tables

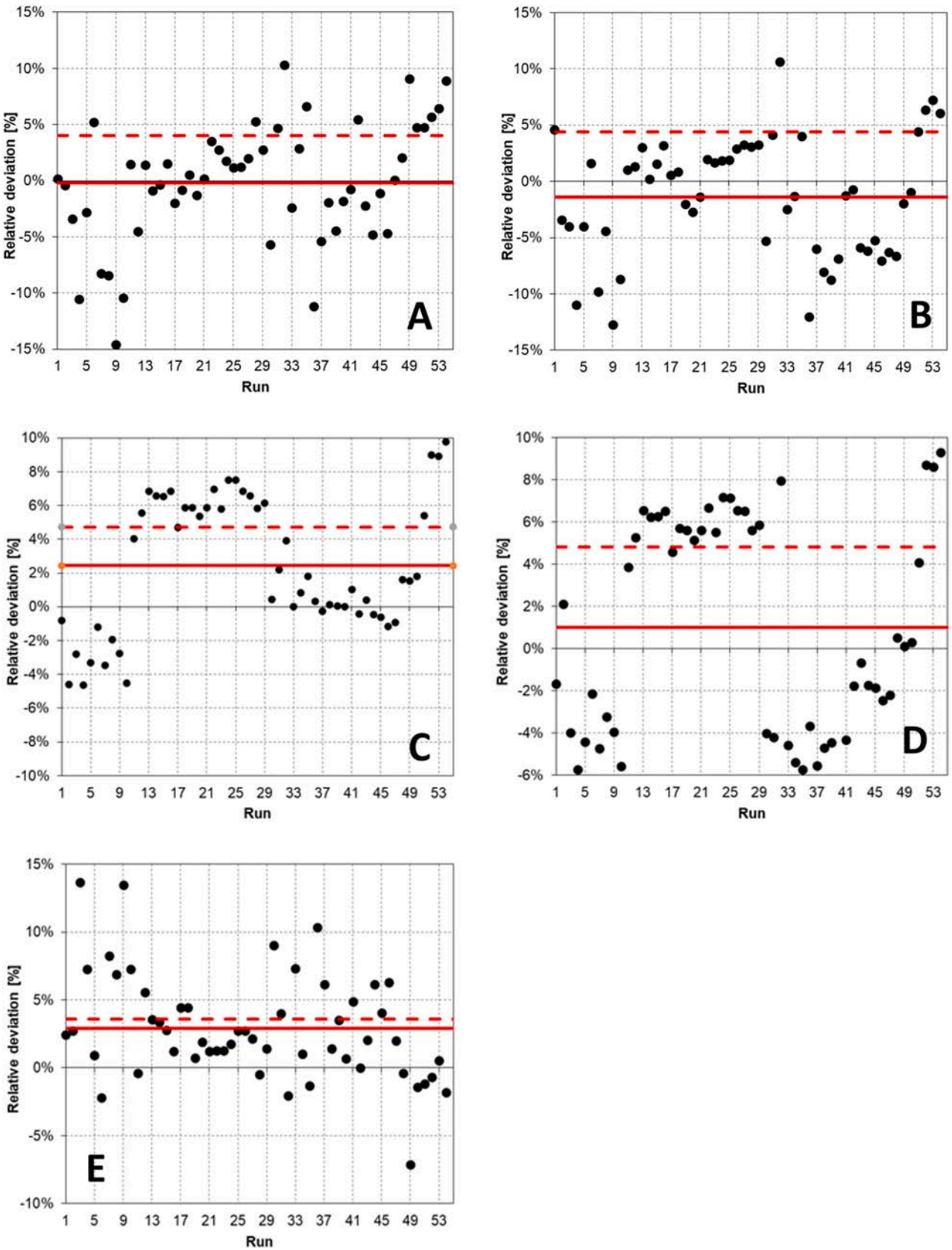

Fig. 5. Relative deviation plots for HS3 Aspen Plus **absorber open-loop** model **validation**: residuals (•), ARD% (—) and AARD% (– -) for (A) CO_2 absorbed flow (measurement CO2M1), (B) CO_2 absorbed flow (measurement CO2M2), (C) temperature profile (liquid), (D) temperature profile (vapor), and (E) rich loading.

Table 4
Outcomes of the **statistical analysis** (experimental data uncertainty and model prediction uncertainty) for the **open-loop** HS3 model **validation** of the **absorber** over Tiller pilot plant data.

Compared output	Model ARD%			Model AARD%			Model STD		
Flue gas CO_2 content	All runs	5.5 vol%	12 vol%	All runs	5.5 vol%	12 vol%	All runs	5.5 vol%	12 vol%
CO_2 captured flow – CO2M1 [kg/h]	−0.23	3.35	−4.42	4.03	3.35	5.63	1.469	0.811	1.808
CO_2 captured flow – CO2M2 [kg/h]	−1.41	2.99	−2.12	4.41	3.73	4.72	1.384	0.914	1.648
T profile – liquid [°C]	2.45	6.37	−0.53	3.71	6.37	1.66	2.380	4.001	1.198
T profile – vapor [°C]	1.02	5.95	−2.97	4.79	6.23	3.43	3.300	4.118	1.718
T profile-liquid (abs. value) [°C]	–	–	–	4.70	6.91	3.06	–	–	–
T profile-vapor (abs. value) [°C]	–	–	–	4.80	6.64	3.44	–	–	–
Rich loading [mol/mol]	2.88	1.63	3.81	3.59	2.10	4.69	0.009	8.1E-5	0.002

list the absolute and relative deviations run-by-run for the open-loop validation for both absorber and stripper.

5.1.4. *Close-loop validation*

Fig. 8 shows the residuals for the closed-loop testing, including the deviations in the estimated CO_2 capture rate and the predicted lean and rich loadings. The values of the AARD%, ARD% and STD for the CO_2 capure rate, lean and rich loading are gathered in Table 7. The close-loop analysis is here limited to ten runs. Table S9 in the Supplementary Material highlights the relative and absolute errors for the main KPIs checked in the closed-loop validation. These ten runs were chosen to cover the domain of interest for the capture plant using HS3 in terms of capture rates, loading and CO_2 gas inlet concentration (Table 6), while we disregarded all the other runs because not relevant for the purpose of validating the model (either too low capture rates or loadings far from the optimal operating conditions). Indeed, the validation of the closed-

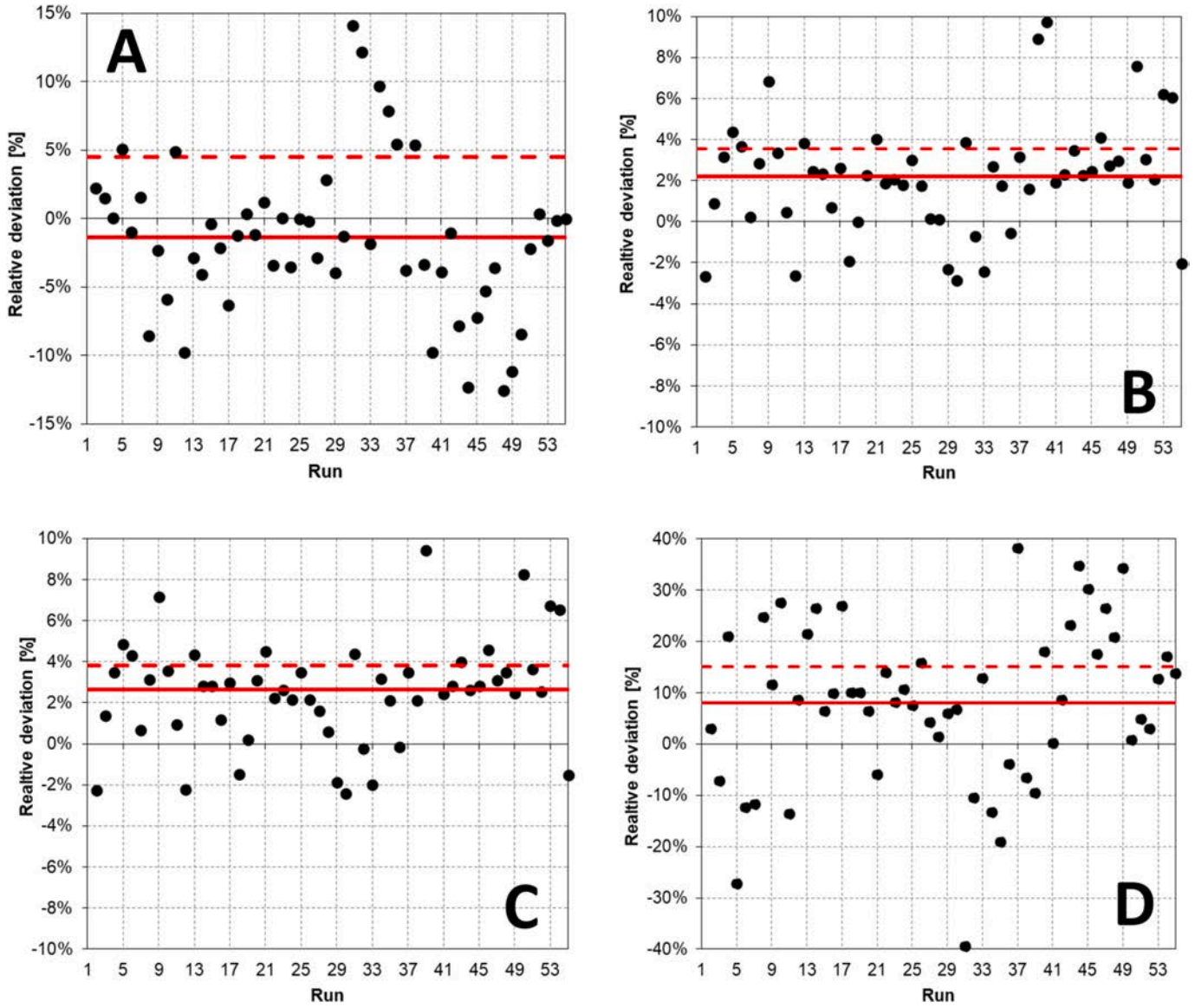

Fig. 6. Relative deviation plots for HS3 Aspen Plus **desorber** model **open-loop validation**: residuals (•), ARD% (—) and AARD% (– -) for (A) CO_2 released flow (CO2M4), (B) temperature profile (liquid), (C) temperature profile (vapor), and (D) lean loading of the regenerated solvent.

Table 5
Outcomes of the **statistical analysis** (model prediction uncertainty) for the **open-loop** HS3 model **validation** of the **stripper** over Tiller pilot plant data.

Compared output	Model ARD%			Model AARD%			Model STD		
Flue gas CO_2 content	All runs	5.5 vol%	12 vol%	All runs	5.5 vol%	12 vol%	All runs	5.5 vol%	12 vol%
CO_2 released flow (CO2M4) [kg/h]	−1.53	−1.61	−0.88	4.30	2.13	5.87	1.574	0.600	2.013
T profile – liquid [°C]	2.17	2.19	2.23	2.84	2.81	2.87	4.467	–	–
T profile – vapor [°C]	2.65	2.52	2.76	3.17	3.05	3.27	4.853	–	–
T profile-liquid (abs. value) [°C]	–	–	–	3.50	3.48	3.52	–	4.307	4.585
T profile-vapor (abs. value) [°C]	–	–	–	3.78	3.65	3.88	–	4.534	5.090
Lean loading [mol/mol]	7.91	10.42	5.57	14.57	12.23	16.99	0.017	0.009	0.013

loop aims at showing the reliability of the proposed model close to the most relevant operating condition, i.e., close to the optimum where the minimum SRD is reached. The experimental SRD reported in Table 6 is calculated by subtracting the plant thermal losses (close to 2 kW) from the provided reboiler duty, and then dividing the obtained thermal input by the flow of CO_2 stripped inside the desorber, the most accurate measurements available in the plant (refer to Section 3.2).

The close-loop simulations confirm the reliability of the model. CO_2 capture rates and loadings are sufficiently aligned with pilot plant observations for each of the ten investigated runs: the maximum discrepancy observed for the CO_2 capture rate is below 6%, while the accurate predictions of both lean and rich loadings ensure a reasonable estimate of the cycling capacity, which is the driving force for CO_2 absorption. The cycling capacity is one of the most significant performance indicators of the solvent because mass transfer, kinetics, and thermodynamic equilibria affect this property of the solvent. The good alignment between measurements and model outcomes consolidates the accuracy of the proposed Aspen model for the HS3 solvent.

5.2. *Sensitivity analysis for process optimization and case study design*

The sensitivity analysis has been tailored to optimized the process layout scketched in Fig. 3 in terms of energy demand. This task has been done to get a preliminary assessment of the carbon capture system using two solvent, i.e., MEA (benchmark) and the new HS3 blend, in an optimized system. In this way, the comparison of the results is unbiased because the two processes are contrasted at their best performance on the same plant. The objective function is the minimization of the specific reboiler duty (SRD), i.e., the energy consumption. This is the target because research is devoted to reduce at least the energy intensity of carbon capture, as remarked in the Introduction. The proposed methodology aims to define the optimal values for the remaining degrees of freedom for the capture plant. The analysed parameters are:

- The solvent lean loading which influences also the liquid-gas ratio (L/G) in the absorber.
- The packing height which impacts the L/G ratio.
- Operating condition for the stripper (pressure and feed stage for the hot rich solvent).
- Water wash design constrained to emissions limitations.

Table S4 gathers the rational and the investigated ranges. The analysed ranges have been set upon prior literature for MEA (Abu-Zahra et al., 2007b) and experimental campaign at Tiller for HS3 solvent. The stopping criteria for each parameter is described in the corresponding paragraph. Remarkably, lean loading, packing height, and L/G ratio are intrinsically entangled because all contribute to determining the thermal duty, thus, the specific reboiler duty (SRD) at fixed capture ratio, i.e., 90% of the fed CO_2. The interconnection between these parameters has been intensively studied in the literature in pilot plants (Brigman et al., 2014) and modelling (Michailos and Gibbins, 2022). Similarly, packing height and stripper pressure are the parameters to be optimized for the regeneration. The pressure is the most relevant parameter because it constrains the reboiler temperature, which affects the thermal

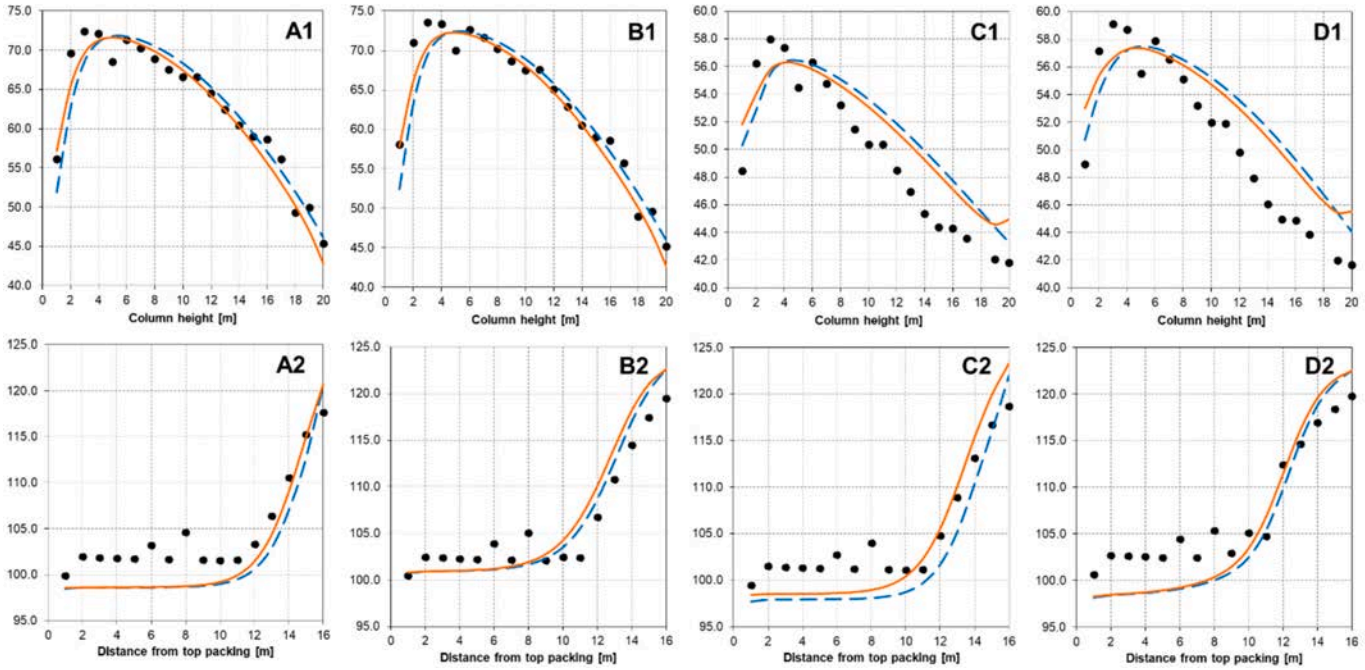

Fig. 7. Examples of temperature profiles inside the absorber (1 –row) and stripper (2 –row) for a CO_2 inlet gas content of 12 mol% (cases A and B) and 5.5 mol% (cases C and D). Experimental data (•) against model prediction: (–) liquid phase temperature and (– -) vapor temperature using the rate-based model.

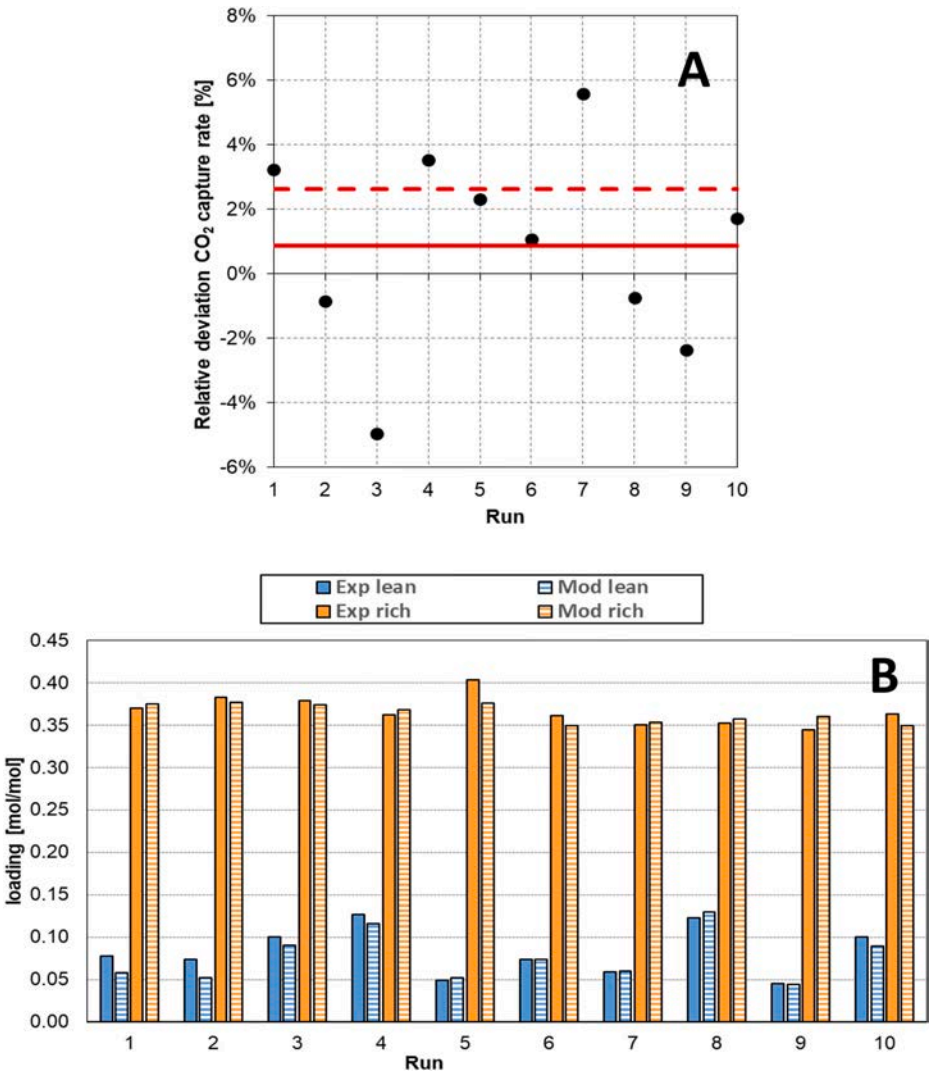

Fig. 8. Results of the Aspen ELECNRTL model **closed-loop validation** over the Tiller pilot plant data: (A) residuals (•), ARD% (—) and AARD% (– -) for the CO2 captured flow and (B) comparison between model-predicted and experimental lean and rich loadings.

Table 6
Characterization of the ten runs chosen for HS3 **close-loop** model **validation** in terms of CO_2 concentration in the fue gas and experimental lean loading, cycling capacity, capture rate, and SRD.

Run	CO_2 conc. [vol%]	Exp. Lean loading [mol/mol]	Exp. Cycling capacity	Exp. Capture rate [%]	Exp. SRD [MJ/kg CO_2]
6	12	0.100	0.279	95.2	3.14
7	12	0.126	0.236	95.0	3.34
9	12	0.049	0.354	98.5	3.12
12	5.5	0.222	0.230	89.1	3.39
19	5.5	0.074	0.288	95.2	3.48
22	5.5	0.046	0.299	90.2	3.77
28	5.5	0.100	0.263	88.2	3.60
39	12	0.073	0.310	90.5	3.06
51	12	0.078	0.292	94.5	3.15
53	5.5	0.058	0.292	90.0	3.58

Table 7
Outcomes of the **statistical analysis** (model prediction uncertainty) for the **close-loop** HS3 model **validation**.

Compared output	Model ARD%	Model AARD%	Model STD
CO_2 capture rate [%]	0.86	2.84	2.86
Rich loading [mol/mol]	0.73	2.59	0.012
Lean loading [mol/mol]	8.74	10.66	0.013

degradation of the solvent. It is a well-established practice to range the solvent regeneration temperature between 115 and 125 °C regardless of the solvent (Dutcher et al., 2015) even though there are solutions to limit solvent thermal degradation (Meng et al., 2022) or recover the solvent from the thermal degraded products (Wang et al., 2015). The reboiler temperature window is also constrained to the steam quality and the integration with power plants. For guaranteeing reduced energy penalty, saturated steam at 130 °C is often considered (Oexmann et al., 2012). Finally, the water wash design was carried out based on current emissions limitations even though they are expected to become more stringent. The cooling water temperature is set to 20 °C which corresponds to the maximum one registered in the of Irving Oil refinery. This has been done for the sake of conservativeness. Nevertheless, the cooling water temperature has a key role to compensate for water loss and keep the water balance. The effect of the cooling water temperature on the energy penalty has been investigated for ammonia-based carbon capture in Linnenberg et al. (2012). The lower the temperature, the lower the energy penalty associated with the carbon capture, especially for ammonia capture where lower temperatures reduces the solvent volatility. However, this is generally valide for amines. This property of the

utility is particularly relevant in warm/tropical regions and/or off-shore applications where cooling may be a challenge (Cruz et al., 2023) as well as for power plants which requires significant quantitites of water (Zhai et al., 2011). Finally, we disregarded the implementation of acid washer to abate volatile amine-degraded products emissions (Edwards et al., 1978) which could shorten the water wash packing but further complicates the process because you need to handle strong acids and account for a water treatment section and solid-wastes disposal (Khakharia et al., 2014).

5.2.1. Lean loading and columns packing heights optimization

Figs. 9 and 10 show the profile of the SRD and liquid-gas (L/G) ratio as a function of the lean loading for different packing heights for MEA and the new HS3 solvent, respectively. The optimal lean loading for MEA is 0.24. This value is in line with pilot scale data collected during a campaign carried out at Technology Centre Mongstad (Norway) and reported by Brigman et al. (2014), as well as with other modelling works under comparable operating conditions (Raynal et al., 2011). H = 12 m is the optimal packing height for simulations with MEA 30 wt%. This condition limits the SRD decrease below 1% with an increment of 2 m column (Fig. 9A).

Similarly, HS3 performances are optimized at significantly lower loadings, in compliance with the higher total amine concentration of the solvent (55 wt% versus 30 wt%) and as expected for second-generation amines (Feron et al., 2020). The energy requirements remain almost flat in a range of loadings between 0.06 and 0.08, whereas they rapidly increase if the loading is slightly reduced from 0.06 to 0.05. This is confirmed by pilot plant observations collected at Tiller. The lean loading of 0.07 has been selected as the final optimal lean loading to keep a safety margin from the a steep SRD increament occurring below 0.06 mol/mol. The select lean loading does not cause a substantial increment of the reboiler duty. The results show that a packing of 18 m (+50% compared to MEA) is required. This result is somehow expected since that the new blend absorbs CO_2 slower than 30 wt% MEA.

Simulations of the CO_2 capture plant at variable stripper packing height (2 m discretization step) are run at fixed absorber packing height and the lean loading to their optimal values presented in the previous section. The results ar plotted in Fig. 11. The optimal packing heights are 10 and 14 meters for MEA and HS3, respectively. The optimization of the packing height followed the same criteria adopted for the absorber.

5.2.2. Feed stage and operating pressure effect in the desorber

Fig. 12 depicts the effect of the feed stage on the Specific Reboiler Duty (SRD). Indeed, even if the column is of packed type, a certain height of packing corresponds to an ideal height of a theoretical stage in trayed columns. The best feed stage minimizes the SRD; thus, the top stage for HS3 and the second stage for MEA.

The SRD as well as the reboiler temperature are collected at different stripper operating pressures, between 1.6 and 2.2 bar. The results are available in Figs. 13 and 14 for MEA and HS3, respectively. As expected, the higher the stripper pressure the lower the SRD, but the higher the corresponding reboiler temperature. The maximum operating pressure that allows not to overcome the selected temperature threshold of 123 °C in the reboiler is equal to 1.9 and 1.8 for MEA and HS3, respectively.

SRD does not show variations above 1% if the lean solvent temperature is varied in a range between 35 °C and 50 °C, which is the typical solvent inlet temperature range considered for these applications (Li et al., 2016). On the other hand, it is anyway important to analyze the effect of the lean solvent temperature on other performance indicators the cooling water and the volatile amine emissions. The lean solvent temperature is responsible for cooling water consumption and amine traces in the treated gas leaving the absorber as depicted in Fig. 15 and Fig. 16. The residual amine content here reported refers to the gas exiting the top of the absorber. Our target is the design of the water-wash packing height to meet the amine emission requirement. This task will be carried out in a second step directly on the optimized plant configuration resulting from this sensitivity analysis.

5.2.3. Water wash analysis for emissions reduction

For what concerns amine emissions, AP emissions are comparable to MEA, while the amount of PRLD is far higher. The PRLD and its degradation products are more volatile than the primary amine (Vevelstad et al., 2023). Amine concentrations significantly affect the design of the water wash section, and the design of this unit is aimed at matching emissions control below imposed threshold values. Based on these considerations, the lean solvent temperature must be tuned to find a compromise between the cooling water consumption (utility) and the amine emissions (constraint), which are both linked to a potentially relevant increase for both investments and operating costs.

Results are reported in Figs. 15 and 16. The cooling water requirements start increasing much more rapidly if the set solvent inlet temperature is below 43 °C. On the other hand, amine emissions grow almost linearly. Therefore, 43 °C is assumed as the optimal feed solvent temperature.

5.2.4. Resume

The optimal operating parameters and the key performance

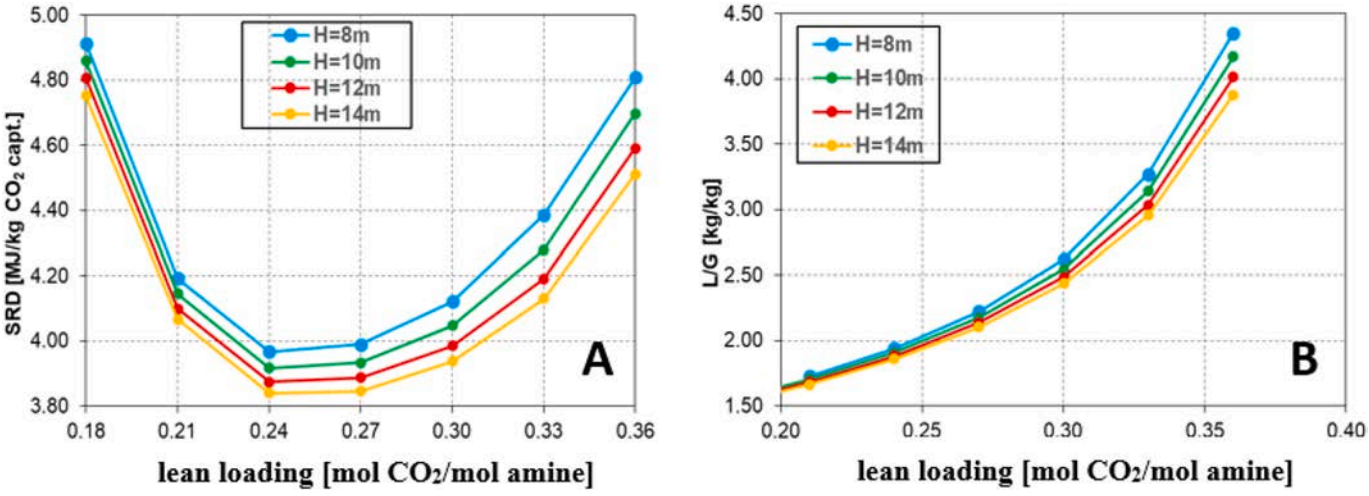

Fig. 9. – SRD (A) and L/G ratio (B) as a function of the lean loading for MEA solvent evaluated at different packing heights: 8 m (light blue), 10 m (green), 12 m (red), and 14 m (orange). (For interpretation of the references to colour in this figure legend, the reader is referred to the Web version of this article.)

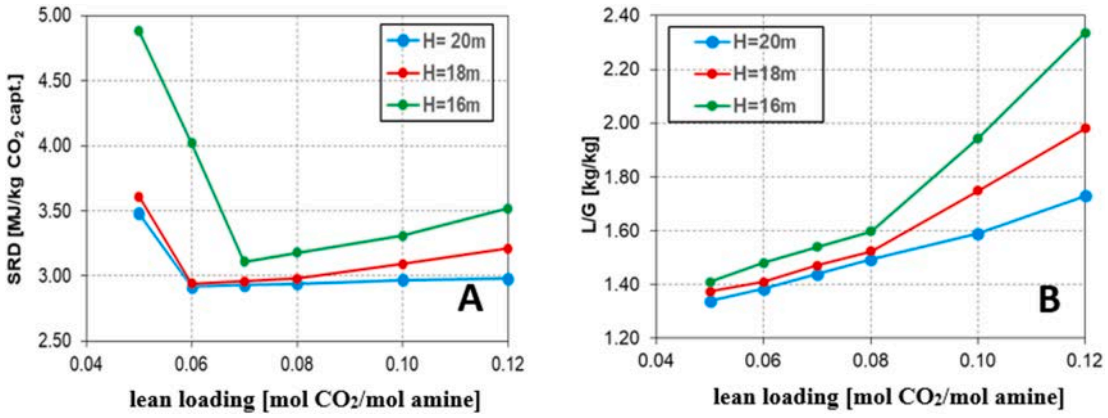

Fig. 10. – SRD (A) and L/G ratio (B) as a function of the lean loading for HS3 solvent evaluated at different packing heights: 20 m (light blue), 18 m (red), 16 m (green), and 14 m (orange). (For interpretation of the references to colour in this figure legend, the reader is referred to the Web version of this article.)

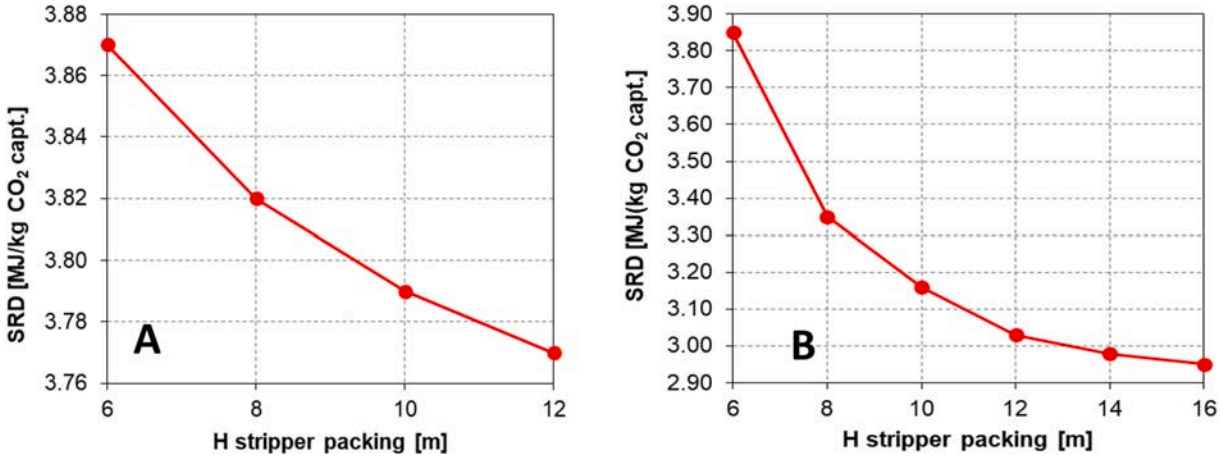

Fig. 11. SRD profiles as a function of the stripper packing height for A) MEA and B) HS3 solvent. Absorber packing height and lean loading are already set at optimal values.

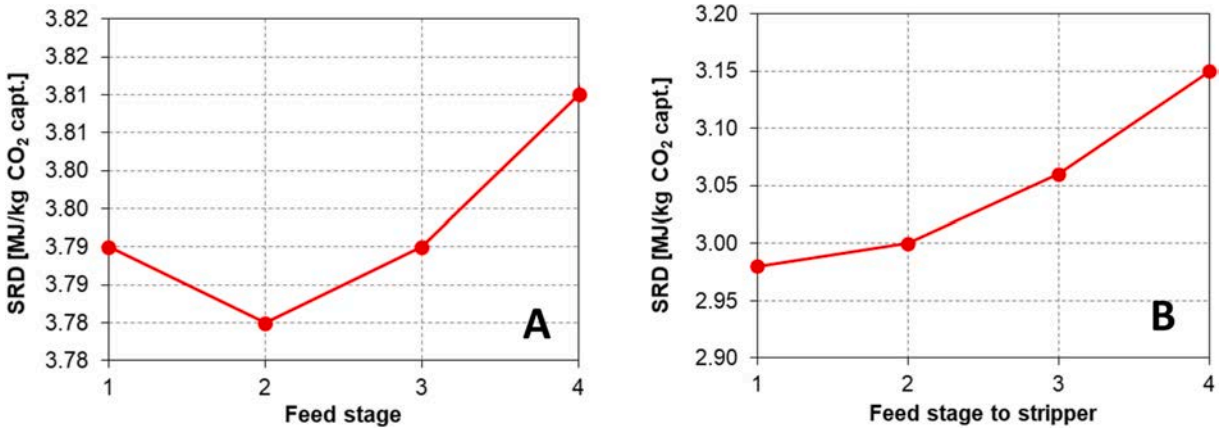

Fig. 12. SRD variation as a function of the rich solvent feed stage to the stripper for A) MEA and B) HS3. Absorber, stripper packing height and lean loading are already set at the optimal values.

indicators (KPIs) resulting from the sensitivity analysis are summarized in Table 8 for both HS3 and MEA. Due to slower kinetics, higher packing heights are necessary for HS3 solvent. On the other hand, the SRD and the L/G ratio for 90% capture ratio are 23% lower with HS3. These results refer to the optimize plants. Moreover, the specific steam requirement (SSR), defined as the net reboiler duty per unit of captured CO_2, can be reduced by over 57% using HS3. The net reboiler duty is the difference between the total thermal energy and the heat recovered from the stacks. The optimal SRD associated to HS3 solvent obtained for the investigated case-study is slightly lower than the corresponding minimum SRD estimated at Tiller plant (see Table 6). This outcome can be explained considering that the Tiller facility is meant as a facility for

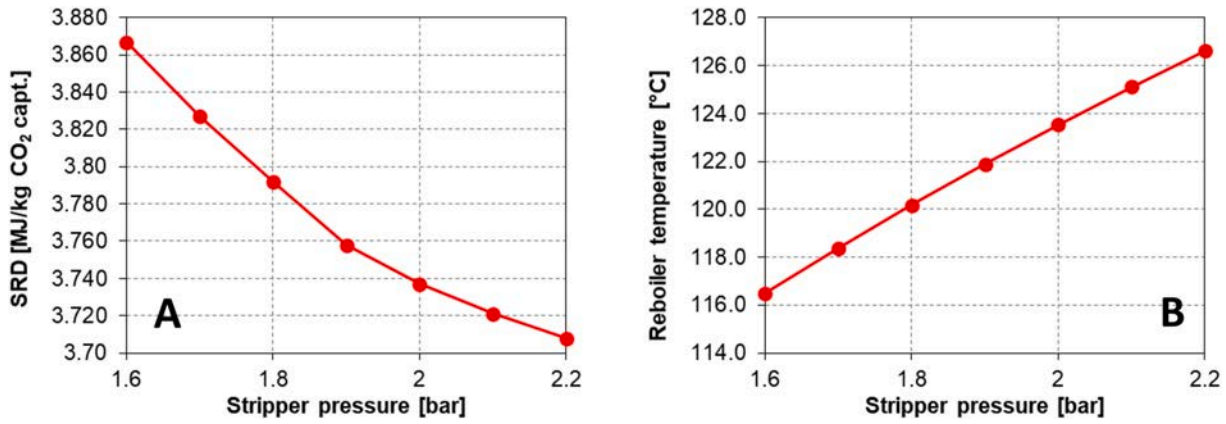

Fig. 13. Plot of A) SRD and B) reboiler temperature as a function of the stripper operating pressure for MEA solvent. Packing heights, lean loading and feed stage to regeneration are set to the optimal values.

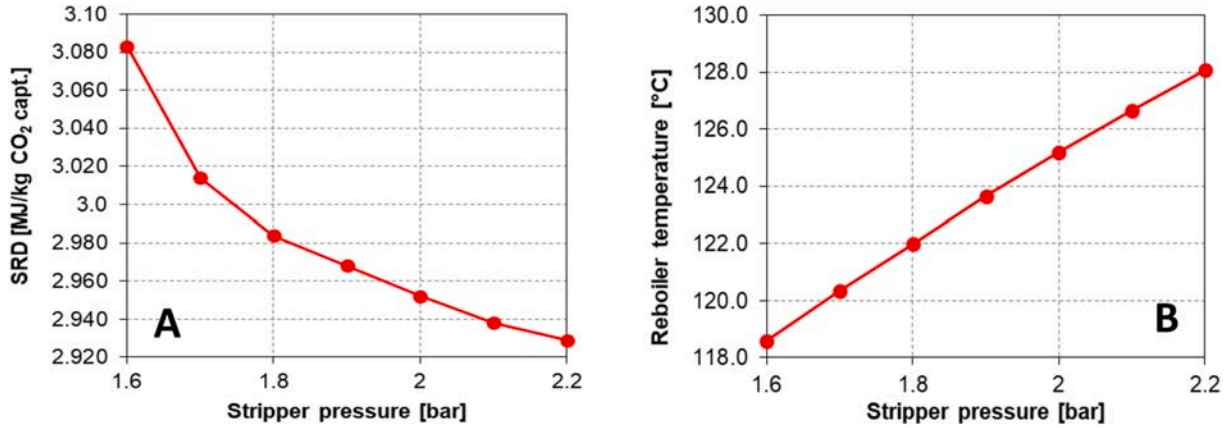

Fig. 14. Plot of A) SRD and B) reboiler temperature as a function of the stripper operating pressure for HS3 solvent. Packing heights, lean loading and feed stage to regeneration are set to the optimal values.

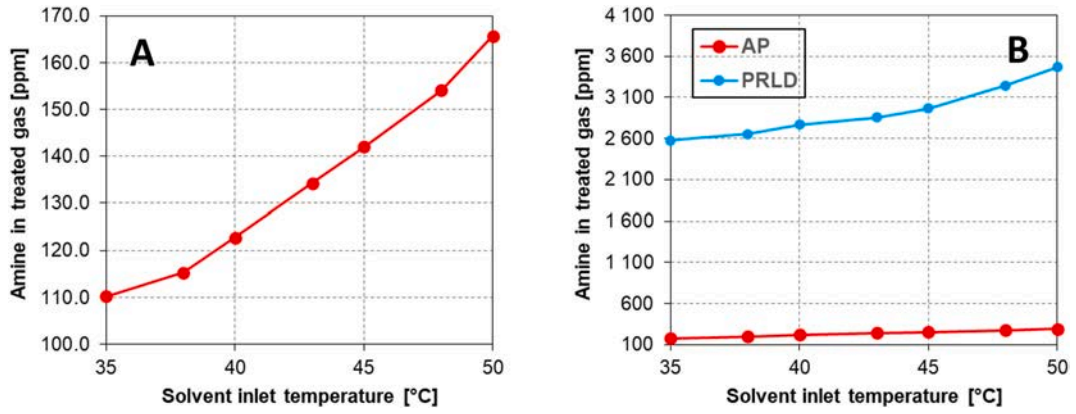

Fig. 15. Residual amine concentration (in ppm vol) in the treated gas at different solvent inlet temperatures using A) MEA and B) HS3 solvent.

solvent testing at given operating conditions and equipment sizing, it is not an optimized plant for a specific application such as the one designed for Irving Whitegate oil refinery. Moreover, the pilot facility is intrinsically associated with temperature and pressure losses (Mejdell et al., 2022), which have been disregarded in the upscaled capture plant design. The heat loss in large-scale facilities is negligible due to the lower exposed external surface/volume ratio as Lawal et al. assumed in modelling and then demonstrated in a large carbon capture plant (Lawal et al., 2012). Finally, the packing implemented at Tiller CO_2Lab (Mellapak 2*X*) is less efficient compared to Mellapak 250*X*, considered for the design of the carbon capture plant in the industrial case study. Mellapak 250*X* has a higher exposed surface to contact the solvent and the flue gas and this helps to reduce the amount of liquid. However, the higher exposed surface and lower empty volume leads to higher pressure drop in Mellapak 250*X*/Y (Park and Øi, 2017). The selection of the optimal structured packing relies on a broader analysis of the column fluidodynamic, gas velocity, flooding conditions based on a detailed and extensive experimental investigation (Wang et al., 2015), which is out of

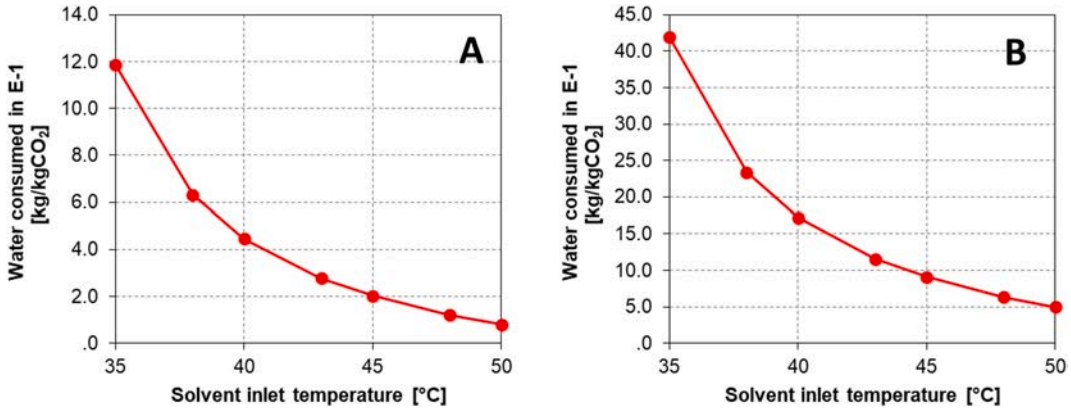

Fig. 16. Cooling water consumption in solvent cooler (E−1) at different solvent inlet temperatures using A) MEA and B) HS3 solvent.

Table 8
Results of the sensitivity analysis for the optimization of MEA and HS3-based CO_2 capture process for the treatment of the Irving oil refinery flue gas.

Optimized parameters	MEA	HS3	KPI	MEA	HS3
Lean loading [mol/mol]	0.24	0.07	L/G [kg/kg]	1.91	1.47
Absorber packing height [m]	12	18	SRD [MJ/kg_{CO2}]	3.77	2.98
Stripper packing height [m]	10	14	SSR [MJ/kg_{CO2}]	1.59	0.68
Desorber feed ideal stage (from top)	2	1			
Desorber pressure [bar]	1.9	1.8			
Lean solvent temperature [°C]	43	43			

the scope of the present work. However, it is worth underling that the selection of the packing, e.g., material and mesh, influences the energy demand, but the effect on the pressure drop under normal run of the absorber and stripper, i.e., proper design and control, is not significant (Lassauce et al., 2014). The packing is supposed to affect the pressure drop that the fan should compensate for, but in Front-End Engineering Design (FEED) studies blower is oversized by default by 25% to account for any unpredictable pressure drops non associated with the packing (Elliott et al., 2022). The scope is to have a margin. In the present study we limited our analysis to Mellapak 2*X* and 250*X* because these are the most used packing for carbon capture applications regardless the solvent composition (Razi et al., 2012). However, Sulzer is going to commercialize an innovative family of packings for carbon capture applications (Lee, 2022). This new structured packing is expected to reduce the pressure drop within columns, but its price is still unknown and it could be more expensive than packings already in use. It is unclear whether the energy saving outweighs/balances the increased investment costs because a detailed analysis is still missing.

5.3. Capture plant performances and energy requirements

This section reports the results of the simulations of the CO_2 capture plant for the treatment of the Irving oil flue gas in Aspen Plus. The simulation was run by setting the optimal operating conditions from the sensitivity analysis. Here, the focus is on the estimate of the main equipment size and on the energy requirements. The results refer to both MEA and HS3, and a comparison between the two solvents based on energy requirements, equipment sizing and key performance indicators is also reported.

5.3.1. MEA case study

The plant treats 280.31 ton/h of Irving Whitegate Oil Refinery flue gas and an additional flow of 27.72 ton/h representing the flue gas generated in the steam boiler. In other words, the boiler increases by 9.8% the total amount of flue gas fed to the carbon capture plant. The average flue gas CO_2 concentration prior the DCC is 7.2 mol%.

990.8 ton/h of cooling water are required to cool down the flue gas from 150 °C assuming a pinch temperature of 3 °C. This significant cooling water consumption is intrinsically determined by the high-temperature gradient between the liquid and gas phase. The large enthalpic content in the gas phase is reflected in a large water consumption to carry out the cooling process. The column has a diameter of 6.8 m (70% flooding). The water stream recovered from the bottom of the unit reaches a temperature of 30 °C, and it must be cooled back to 25 °C by means of cooling water before being recirculated to the DCC. Being the flue gas water content higher with respect to the water saturation point, part of the water contained in the flue gas condenses inside the DCC. For this reason, 0.5% of the water flow recovered at the bottom is purged from the cooling water loop. This purge corresponds to a flow of 21.22 ton/h, and it is made up of almost pure water, with only traces of dissolved CO_2 (44 ppm), N_2 (9 ppm) and O_2 (0.9 ppm). Even if the purity level of this water could justify its use as a make-up stream in the water-wash loop to reduce fresh water consumption, this integration is not proposed in this work to avoid issues arising from the possible accumulation of impurities leading to a lower efficiency of the washing section. The CO_2 concentration in the saturated flue gas increases to 7.98 mol% owing to a partial condensiation of the water in the DCC. The increment of the CO_2 partial pressure benefits the capture process efficiency.

The fan is designed to overcome the total pressure drop occurring on the flue gas side from the preliminary heat recovery until the top of the water-wash section. To consider a safety margin, the treated gas outlet pressure has been set to 1.05 bar. Based on the estimated pressure losses, the fan must compress the flue gas to 1.1 bar, consuming 1.845 MW_{el}. The outlet gas reaches a temperature of 50.41 °C (feed temperature to the absorber).

The solvent flow required to capture the 90% of the CO_2 content in the flue gas entering the absorber is 577.8 ton/h, corresponding to an L/G ratio equal to 1.91 and to a specific solvent flow of 18.39 $ton_{solvent}/ton_{CO2\ capt}$. The solvent enriches CO_2 along the column and reaches a rich loading of 0.506. Therefore, the available cycling capacity is about 0.266 mol/mol amine (1.06 $mol_{CO2}/kg_{solvent}$), compliant with the literature (Knuutila et al., 2019). The column has a packing height of 12 m, as stated from the sensitivity analysis, and a diameter of 5.86 m. Fig. 17 shows the temperature profile and the variation of the CO_2 mole fraction in the vapor phase inside the column. The temperature profile is in accordance with the theory of exothermic reactions and compliant with experimental observations on plants operating with MEA in two dependent works by Montañés et al. (2017) and Nookuea et al. (2016). At the bottom of the column, the vapor temperature decreases owing to the water evaporation occurring inside the column as a result of exothermic reactions between CO_2 and MEA (Putta et al., 2017).

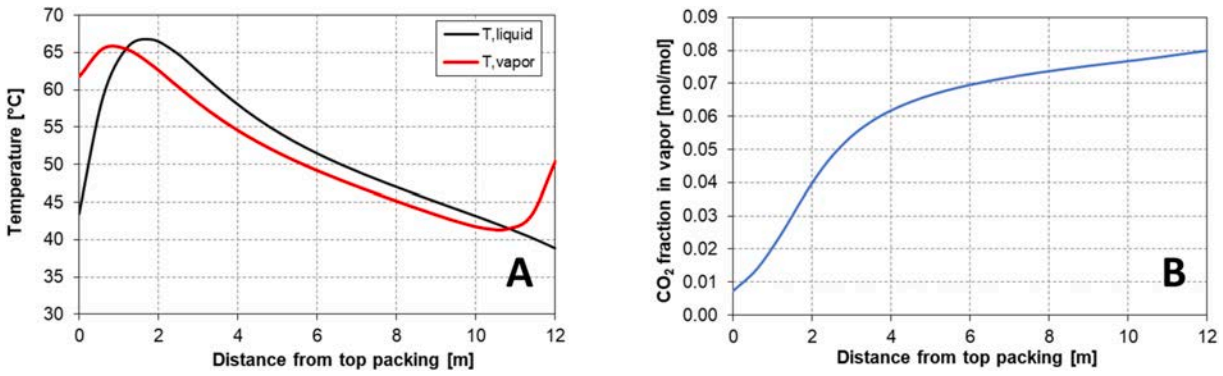

Fig. 17. A) Temperature profile and B) CO_2 content in the vapor phase profile inside the absorber. Results from the simulation in Aspen Plus using MEA default model.

693 ton/h (22.1 $ton_{CW}/ton_{CO2\ capt}$) is the maximum flow of cooling water (CW) to stay below 70% flooding condition (design constraint) in the water wash (WW). The packing height is 2.15 m to guarantee a residual MEA content of 5 ppm in the treated gas. The chart in Fig. 18 tracks the mole fraction of MEA in the vapor phase along the WW packing height to meet the outlet specification.

The rich solvent is withdrawn from the sump of the absorber and pumped to 4.25 bar to overcome the pressure drops of 0.35 bar in HR-11 and the static pressure owing to the stripper elevation (20 m). The rich solvent is preheated in a counter-current cross-heat exchanger before entering the desorber. This solution allows to recover 38.19 MW of heat, thus significantly reducing the energy requirements inside the stripper itself. The preheated rich solvent stream reaches 112.57 °C, while the lean solvent is cooled down to 49 °C. This provides an additional beneficial effect on the overall cooling water consumption in the plant, since only a limited external cooling duty still needs to be provided to further cool the lean solvent down to the absorber inlet temperature.

The stripper releases the CO_2 absorbed in the solvent so that the original lean loading of 0.24 is re-established and the solvent is recirculated to the absorber. The stripper design suggested a packing height of 10 m and a diameter of 3.12 m. The condenser and reboiler duties are 10.51 and 33.05 MW, respectively. Therefore, the specific reboiler duty (SRD) is 3.78 $MJ/kg_{CO2\ capt}$. This value is aligned with prior literature and simulation work using MEA (Abu-Zahra et al., 2007b). Fig. 19 depicts the temperature profile within the stripper and the CO_2 content in the gas phase.

The released CO_2 flow is equal to 31.42 ton/h. The CO_2-rich stream recovered from the stripper has a molar purity of 97.7% on a wet basis

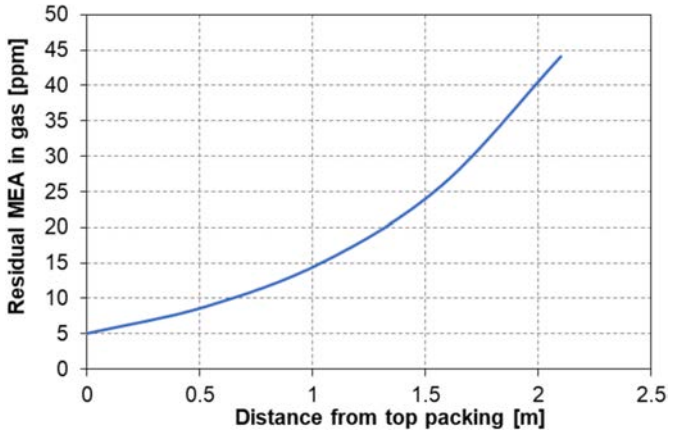

Fig. 18. Progressive reduction of the residual MEA content in the treated flue gas at increasing water wash packing heigh. Results from the Aspen Plus simulation using MEA default package.

(thanks to water condensation at 30 °C in the top knock-out drum, not reported in Fig. 19). The remaining 2.3% is water. MEA content is negligible (order of 10^{-11}), and traces of dissolved nitrogen and oxygen (a few ppms) are present. The residual water is removed during the compression stages (not considered in the present work). This means that the process allows the recovery of high-quality CO_2. Remarkably, the obtained CO_2 purity is another important index beside the energy requirements for a comprehensive comparison between MEA and HS3.

A recap of the sizing for the main unit operations is available in Table 9. The energy and utilities demand (including steam, electricity and cooling water) are gathered in Table 10. Solvent regeneration (steam) and amine abatement (cooling water in the WW) are responsible for most of the utility demand. However, it is worth pointing out that the heat recovery system proposed in Section 4.2 (18.17 MW_{th} recovered) allows reducing the reboiler duty by over 55% (see Table 11).

Therefore, even if the specific reboiler duty is 3.78 MJ/kg CO_2, the steam boiler must provide only 14.88 MW (1.70 $MJ_{th}/kg_{CO2\ capt}$). Hence, the actual demand for steam (saturated at 130 °C) is 24.6 ton/h, corresponding to 0.78 $ton/ton_{CO2capt}$.

Looking at the electricity consumption, the fan is responsible for the largest energy consumption, i.e., 91% of the overall electricity requirements. The large electricity demand is due to the larger pressure drop occurring in the heat exchanger network for heat integration. Although the energy recovery saves up to 55% of the energy demand for solvent regeneration, the exchangers increase the pressure drops on the gas side by 50% with respect to the baseline process.

The cooling water is a minor concern thanks to its low cost. As expected, the main cooling water consumption occurs inside the DCC and WW loops because of the high circulating flow rates on the process side. For the DCC, a large recirculation is needed to cool down from 150 °C to 28 °C large volumes of hot flue gas, while, in the water wash (WW), the cooling water recirculation is set to abate the MEA emissions by legislative limits. An acid washer could be accounted for to minimize the washer volume, but in this case, waste disposal becomes a relevant concern and an additional cost item. Nevertheless, the capital expenses grow due to the construction materials used. For these reasons, this solution has not been considered in the current assessment. Acid washer will be more appealing when emissions limits will become more stringent.

5.3.2. *HS3 case study*

This section reports the results for the same plant run with HS3 blend. For this case study, we have to include an additional flow of 11.63 ton/h (against 27.72 ton/h in MEA case study) from the steam boiler. Compared to the MEA-based plant, the extra flue gas from the steam boiler is 56% less. The flue gas from the boiler represents only 4.27% of the total gas flow to be treated, and 4.7% of the CO_2 fed to the capture plant.

The amount of cooling water required to cool down the flue gas from

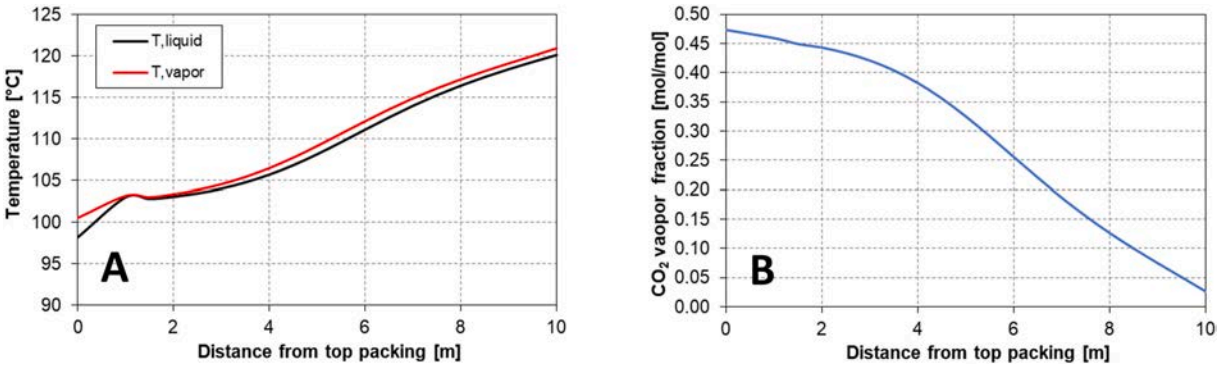

Fig. 19. A) Temperature profile and B) CO_2 content in the vapor phase profile inside the desorber. Results from the simulation in Aspen Plus using MEA default model.

Table 9
Equipment size: diameters and packing heights of the main towers.

Column	Diameter [m]	Packed height [m]
DCC	6.8	3.0
Absorber	5.86	12.0
WW	5.86	2.1
Stripper	3.12	10.0

Table 10
Summary of all the duties (in MW) of the MEA-based CO_2 capture plant.

Equipment	Utility	Duty [MW]
Reboiler (E−3)	Steam	33.05
Fan (C-1)	Electricity	1.85
Pump P-1	Electricity	0.05
Pump P-2	Electricity	0.03
Pump P-3	Electricity	0.06
Pump P-4	Electricity	0.04
Cooler E−1	Cooling water	3.08
Condenser E−2	Cooling water	10.51
Cooler E−4	Cooling water	25.37
Cooler E−5	Cooling water	20.61

Table 11
Summary of total and specific reboiler duties and portion of the duty to be provided by an external heat source (**MEA caae study**).

Duty	Value
Reboiler duty [MW]	33.05
External duty [MW]	14.88
SRD [MJ/kg CO_2]	3.78
SSR [MJ/kg CO_2]	1.70

150 °C to 28 °C is 934.8 ton/h. The DCC diameter is 6.5 m. Since the flue gas water content is higher with respect to the water saturation condition at 28 °C, part of the water contained in the flue gas condenses inside the DCC as mentioned for the MEA case study. For this reason, 2.1% of the water flow recovered at the bottom is purged from the cooling water loop. This purge corresponds to 19.9 ton/h (0.71 ton/$ton_{CO2capt}$), and it is made up almost by pure water, with only traces of disoolved CO_2 (26 ppm mol), N_2 (7 ppm) and O_2 (26 ppm). The purge composition is comparable to the one obtained using MEA, and the same considerations on its potential internal recycle still hold.

The criteria adopted for the pressure drops estimation are similar to the ones adopted for MEA for the sake of consistency. Based on the estimated pressure losses, the fan must compress the flue gas to 1.125 bar, with an electricity consumption of 1.89 MW. The increase in the pressure drop occurs both in the absorber and in the WW, and it is caused by the higher packing height. The outlet gas reaches a temperature of 52.76 °C, which is close to the optimal feed temperature to the absorber for HS3 solvent, and it favors the kinetics.

The solvent flow required to capture 90% of the CO_2 content in the flue gas entering the absorber is 438.3 ton/h, corresponding to an L/G ratio of 1.47 and to a specific solvent flow of 14.87 $ton_{solvent}/ton_{CO2\ capt}$. At the fixed capture ratio of 90% and the same inlet conditions, HS3 reduces by 23% the solvent circulating flow compared to MEA. The solvent enriches in CO_2 along the column and reaches a rich loading of 0.357. Therefore, the available cycling capacity is 0.287 mol/mol amine (1.08 $mol_{CO2}/kg_{solvent}$), which is 8% higher with respect to the cycling capacity obtained for MEA. This observation is compliant with the reduction observed in the specific solvent flow requirement. The column has a packing height of 18 m, as stated in the sensitivity analysis, and its diameter is 5.6 m.

Fig. 20 depicts the temperature profile and the variation of the CO_2 mole fraction in the vapor phase inside the column. The profile is aligned with experimental observations collected on the Tiller plant. The temperature profile inside the column shows a peak temperature which is comparable to the one estimated for MEA.

A packing height of 4.9 m for the WW is necessary to reach a residual total amine content (sum of AP and PRLD) in the treated gas of 5 p.m. This is undoubtedly a disadvantage related to the innovative solvent, since a more than double WW packing height is expected to impact the capital cost. The higher volatility of PRLD, compared to MEA, determines the increment of the packing height required for the WW. Indeed, while AP and MEA have similar vapor pressures at 60 °C (representative of the operating conditions inside the column), PRLD has a significantly higher vapor pressure resulting in larger amine evaporation within the column and one order of magnitude higher residual PRLD content in the treated gas leaving the absorber itself. In fact, the vapor pressure obtained using the Antoine equation implemented in Aspen Plus® for the three amines is 1.52 mbar, 2.24 mbar and 8.1 mbar for MEA, AP and PRLD, respectively.

The chart in Fig. 21 tracks the mole fraction of HS3 constituents in the gas phase along the WW packing height until it reaches the specified threshold. A discretization step of 1 m packing was considered for this analysis.

The rich solvent withdrawn from the bottom of the absorber is pumped to 4.95 bar. This pressure is 0.8 bar higher with respect to the one imposed for the simulation with MEA because of the higher elevation of the stripper, which is 4 m taller than in MEA case study. The rich solvent is preheated to 109.2 °C before entering the desorber, while the hot lean solvent is cooled down from 122 °C to 59.2 °C. The heat recovery is lower than the one obtainable using MEA since the rich solvent leaves the absorber at a higher temperature (42.23 °C) and also the mass flow processed in the cross-heat exchanger is significantly lower. Consequently, also the heat exchanger looks to be more compact (less volume, and less tubes in the bundle).

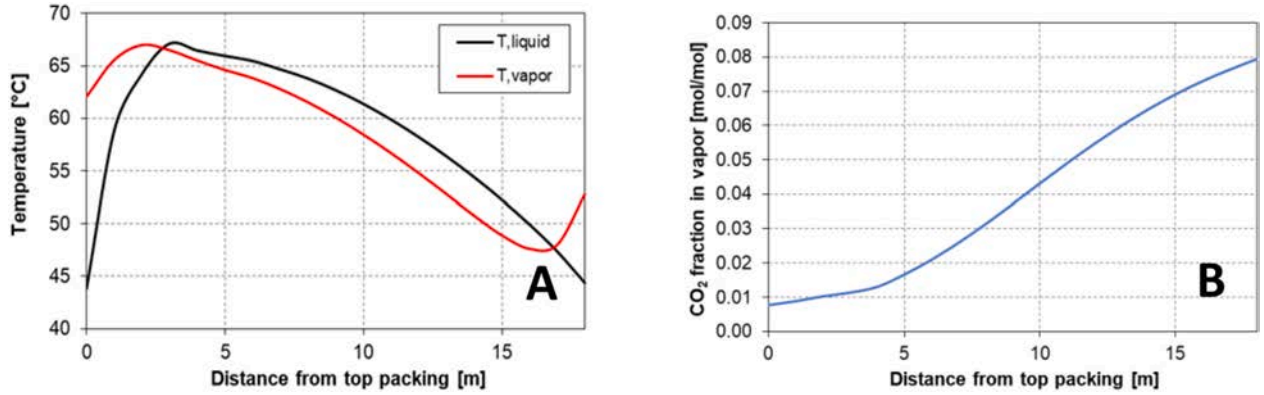

Fig. 20. A) Temperature profile, and B) CO_2 content in the vapor phase profile inside the absorber. Results from the simulation in Aspen Plus using the HS3 model developed in this work.

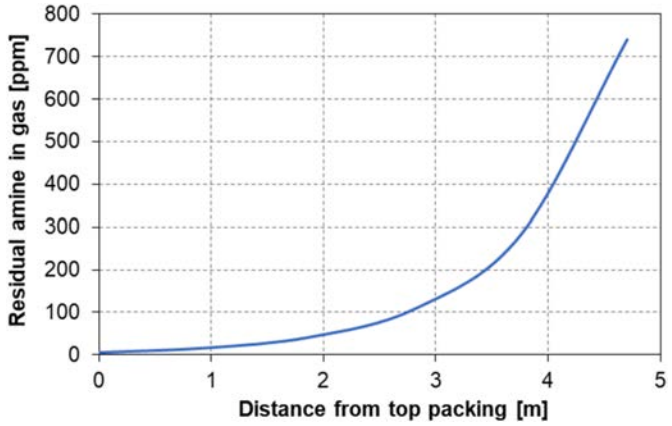

Fig. 21. – Progressive reduction of the residual total amines content in the treated flue gas at increasing water wash packing heigh. Results from the Aspen Plus simulation using the HS3 model developed in this work.

The stripper releases the CO_2 absorbed in the solvent so that the original lean loading of 0.07 is restored and the solvent is ready for recirculation. This column has a packing height of 14 m (4 m higher with respect to MEA plant), while the estimated required diameter is 2.69 m (−14%). The condenser and reboiler duties are 5.73 and 24.45 MW, respectively. Therefore, the specific reboiler duty is 2.98 MJ/$kg_{CO2\ capt}$, with an appreciable reduction by 21% with respect to the SRD calculated for the benchmark MEA. Details of the temperature profile inside the column as well as the variation of the CO_2 content (vol%) are drawn in Fig. 22.

The released CO_2 flow is equal to 29.49 ton/h, lower with respect to total the CO_2 recovered in the simulation with the benchmark solvent due to the lower flue gas flow treated from the steam boiler, since the additional flue gas generated in the NG-fired steam boiler is substantially lower. It is important to underline that the CO_2-rich stream recovered from the stripper has a molar purity of 97.6% on a wet basis, which is comparable to the purity associated with the benchmark operation. Thus, from the CO_2 product stream quality point of view the two solvents show the same features.

Table 12 reports the columns sizing, while Table 13 and Table 14 gather the energy demand and KPIs, respectively. The duty associated to external steam consumption for HS3 solvent regeneration is almost 58% lower with respect to the one calculated for MEA. Indeed, the steam

Table 12
Equipment size: diameters and packing heights of the main towers.

Column	Diameter [m]	Packed height [m]
DCC	6.50	3.0
Absorber	5.60	18.0
WW	5.60	4.9
Stripper	2.69	14.0

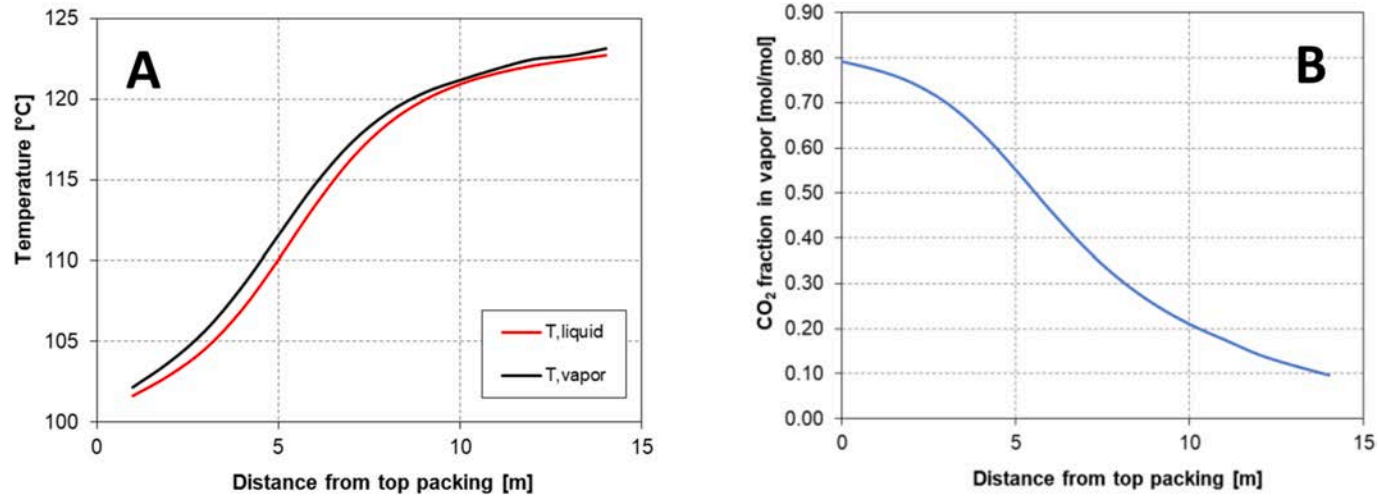

Fig. 22. – A) Temperature profile and B) CO_2 content in the vapor phase profile inside the desorber. Results from the simulation in Aspen Plus using the HS3 model developed in this work.

Table 13
Summary of all the duties (in MW) of the HS3-based CO_2 capture plant.

Equipment	Utility	Duty [MW]
Reboiler (E−3)	Steam	24.45
Fan (C-1)	Electricity	1.89
Pump P-1	Electricity	0.04
Pump P-2	Electricity	0.04
Pump P-3	Electricity	0.05
Pump P-4	Electricity	0.02
Cooler E−1	Cooling water	5.82
Condenser E−2	Cooling water	5.73
Cooler E−4	Cooling water	23.87
Cooler E−5	Cooling water	14.04

Table 14
Summary of total and specific reboiler duties and portion of the duty to be provided by an external heat source (**HS3 case study**).

Duty	Value
Reboiler duty [MW]	24.45
External duty [MW]	6.28
SRD [MJ/kg CO_2]	2.98
SSR [MJ/kg CO_2]	0.77

boiler consume 6.28 MW to produce 10.4 ton/h of steam. The heat recovery exchangers network benefits to reduce the steam consumption. The corresponding SSR = 0.77 MJ_{th}/kg_{CO2} confirms that the energy recovery allows to save almost 75% of the total reboiler duty.

The fan and pumps electricity demands are slightly increased with respect to the MEA-based capture plant. Although the electrical energy for the blower is lower due to the reduced amount of treated flue gas, the pressure drops in the packed bed are higher because of the increased packings height to achieve the assigned capture rate (90%) and reduce the emission to the atmosphere below legislation limits. These two effects are almost compensating one each.

5.3.3. Comparison between HS3 and MEA

A list of the main advantages and disadvantages of HS3 with respect to the benchmark CO_2 capture solvent is reported in Table 15, based on the observations on the results presented in the last two sections and summarized in Table 16. The comparison leads to the conclusion that HS3 allows a significant reduction in the energy requirements (both SRD and SSR), which is expected to impact the operating costs. For what concerns the equipment sizing, it is necessary to balance two opposite effects. On the one hand, the lower circulating solvent flows guarantee the need for lower diameters of the columns (absorber, water wash and stripper) and heat exchangers area. On the other hand, a relevant increase in the packing heights of all the columns must be taken into account due to the slower kinetics.

A cost estimate is necessary to turn this qualitative comparison into a quantitative techno-economic assessment of the expected benefits arising from the implementation of the new HS3 solvent on a large-scale CO_2 capture application. However, this work limits the discussion to equipment sizing and energy analysis. The comparative techno-economic assessment is not included, since it will be the core of a forthcoming assessment and publication.

6. Conclusions

A full model including thermodynamics equilibrium, kinetics and mass transfer has been developed for the novel HS3 amine blend in Aspen Plus V11.0. The proposed model has been validated both on lab-scale and high-quality pilot-scale data covering the entire temperature, loading, and CO_2 capture ranges of interest for industrial-scale CO_2 capture applications. The model can predict all the main KPIs of the carbon capture process with an overall AARD% lower than 5%. This outcome proves that the model can be considered sufficiently reliable for scale-up and techno-economic assessment purposes.

The model shows higher accuracy in predicting the CO_2 captured and released flow as well as the CO_2 loadings when dealing with a low-concentrated flue gas. On average, the model shows a double STD associated to the prediction of the CO_2 flow captured in the absorber and the CO_2 flow released in the stripper when a 12 vol% CO_2 gas is treated rather than a 5.5 vol% CO_2 gas. However, the AARD% associated to the

Table 15
Summary of the main advantages and disadvantages of HS3 solvent with respect to benchmark MEA according to the results of the equipment sizing and energy requirements analysis.

HS3 advantages	HS3 disadvantages	Equal performance
24% lower solvent flow and 19% lower L/G (1.62 vs 1.995)	Slower kinetics	Purity of the product CO_2 stream (>97%)
26% lower reboiler duty (24.45 MW vs 33.05 MW)	Higher column packing heights (+50% for absorber)	Comparable pressure drops and specific electricity requirements
Lower specific energy requirements (21% lower SRD)	Higher volatility (higher water wash section packing required)	Same plant layout (same number and type of unit operations), thus, the revamping of the existing MEA plants looks to be feasible.
Higher fraction of steam generated in the preliminary heat recovery section with respect to the total reboiler steam requirements (45% lower SSR)	Higher initial solvent cost (PRLD is the most expensive component in the blend)	
Lower absorber and stripper diameters (−4.4% and −13.8%, respectively)	Amine loss for the blend is similar to MEA. PRLD (the tertiary amine) degrades thermally to volatile pyrrolidine.	
Lower heat exchange surfaces due to both lower flue gas flow treated and lower solvent circulating flow (i.e., −24.6% for the lean-rich recovery exchanger)		

Table 16
Recap of equipment sizing and performance assessment obtained from the simulation of the optimized CO_2 capture plant for the treatment of Irving Whitegate oil refinery flue gas using benchmark MEA and novel HS3 blend, respectively.

Parameter	HS3	MEA	HS3 variation
Flue gas from boiler [t/h]	11.63	27.72	−58.0%
Flue gas from stacks [t/h]	280.31	280.31	
Cycling capacity [mol_{CO2}/mol_{amines}]	0.287	0.266	+7.9%
L/G [kg/kg]	1.62	1.995	−18.8%
Absorber packing height [m]	18	10	+80.0%
Absorber diameter [m]	5.60	5.86	−4.4%
Water wash height [m]	4.9	2.1	+133.3%
Stripper packing height [m]	12	8	+50.0%
Stripper diameter [m]	2.69	3.12	−13.8%
Reboiler duty [MW_{th}]	24.45	33.05	−26.0%
SRD [$MJ_{th}/kg_{CO2\ capt}$]	2.98	3.78	−21.2%
SSR [$MJ_{th}/kg_{CO2\ capt}$]	0.77	1.70	−54.7%
Percentage of the regeneration thermal duty recovered from flue gas [%]	74.3	55.0	+35.1%
Cooling water in DCC [t/h]	934.8	990.8	−5.7%
Cooling water in WW [t/h]	445.8	644.0	−30.8%

worst-performing scenario (treatment of a 12 vol% CO_2 flue gas) is still below 7% for all the investigated KPIs. The model is further validated on a close-loop, showing a prediction of both capture rates and lean and rich loadings which is compliant with the corresponding pilot-scale tests for all the investigated runs.

The validated model has been used to study a large-scale application, namely the treatment of an oil refinery flue gas. To this aim, a dedicated process flowsheet has been designed for the this specific application, and a sensitivity analysis has been carried out to optimize its operating conditions. The same industrial case has been simulated both using the novel HS3 blend and reference MEA 30 wt% as the benchmark solvent. Results show that the HS3 solvent allows reducing both the energy requirements of the CO_2 capture process (21% lower SRD with respect to the benchmark) and the required circulating solvent flow per unit of captured CO_2 (19% lower with respect to the benchmark). When the internal heat recovery from the hot flue gas stacks is maximised, the external steam requirement drops from 45% to 26% when benchmark MEA is replaced with the HS3 blend. The drawbacks of the new blend are the slower kinetics and the higher overall solvent volatility.

CRediT authorship contribution statement

Matteo Gilardi: Conceptualization, Data curation, Formal analysis, Investigation, Methodology, Software, Validation, Visualization, Writing – original draft, Writing – review & editing. **Filippo Bisotti:** Data curation, Formal analysis, Investigation, Methodology, Software, Validation, Visualization, Writing – original draft, Writing – review & editing. **Hanna K. Knuutila:** Conceptualization, Formal analysis, Methodology, Supervision, Writing – original draft, Writing – review & editing. **Davide Bonalumi:** Conceptualization, Resources, Supervision, Writing – original draft, Writing – review & editing.

Declaration of competing interest

The authors declare that they have no known competing financial interests or personal relationships that could have appeared to influence the work reported in this paper.

Data availability

The data that has been used will be uploaded and available to public at the EU Commission REALISE CCUS webpage (https://cordis.europa.eu/project/id/884266).

Acknowledgement

Matteo Gilardi and Filippo Bisotti would like to thank Olaf Trygve Berglihn (SINTEF) for the useful discussions and suggestions on the implementation of customized ELECNRTL models in Aspen Plus. The authors acknowledge Prof. Stefania Moioli (Politecnico di Milano) for her hints to set up the model validation. The authors are also grateful to Andrew Tobiesen (SINTEF) for his support while developing the model. The work is part of the REALISE project. The project received funding from the European Union's Horizon 2020 research and innovation (RIA) programme under grant agreement No 884266 (https://cordis.europa.eu/project/id/884266).

List of acronyms used

AARD	Absolute Average Relative Deviation
ABS	Absorber
AP	3-amino-1-propanol
ARD	Average Relative Deviation
CW	Cooling Water
DCC	Direct Contact Cooler
DES	Desorber/stripper
ELECNRTL	Electrolyte Non-Random Two Liquids
HR	Heat Recovery (heat exchanger)
KPIs	Key Performance Indicators
L/G	Liquid-Gas (ratio)
MDEA	Methyldiethanolamine
MEA	Monoethanolamine
NRTL	Non-Random Two Liquids
PRLD	1-(2-hydroxyethyl)-pyrrolidine
SRD	Specific Reboiler Duty
SSR	Specific Steam Requirement
STD	Standard Deviation
TRL	Technology Readiness Level
VLE	Vapor-Liquid Equilibria
WW	Water Wash

Appendix A. Supplementary data

Supplementary data to this article can be found online at https://doi.org/10.1016/j.jclepro.2024.141394.

References

Abu-Zahra, M.R.M., Niederer, J.P.M., Feron, P.H.M., Versteeg, G.F., 2007a. CO2 capture from power plants: Part II. A parametric study of the economical performance based on mono-ethanolamine. Int. J. Greenh. Gas Control 1, 135–142. https://doi.org/10.1016/S1750-5836(07)00032-1.

Abu-Zahra, M.R.M., Schneiders, L.H.J., Niederer, J.P.M., Feron, P.H.M., Versteeg, G.F., 2007b. CO2 capture from power plants. Part I. A parametric study of the technical performance based on monoethanolamine. Int. J. Greenh. Gas Control 1, 37–46. https://doi.org/10.1016/S1750-5836(06)00007-7.

Adu, E., Zhang, Y.D., Liu, D., Tontiwachwuthikul, P., 2020. Parametric process design and economic analysis of post-combustion CO2 capture and compression for coal- and natural gas-fired power plants. Energies 13, 2519. https://doi.org/10.3390/en13102519.

Antonini, C., Pérez-Calvo, J.-F., van der Spek, M., Mazzotti, M., 2021. Optimal design of an MDEA CO2 capture plant for low-carbon hydrogen production — a rigorous process optimization approach. Separ. Purif. Technol. 279, 119715 https://doi.org/10.1016/j.seppur.2021.119715.

Arias, A.M., Mores, P.L., Scenna, N.J., Mussati, S.F., 2016. Optimal design and sensitivity analysis of post-combustion CO2 capture process by chemical absorption with amines. J. Clean. Prod. 115, 315–331. https://doi.org/10.1016/j.jclepro.2015.12.056.

Aspen Plus®, 2019. Aspen Plus® V11.0 Documentation.

Bains, P., Psarras, P., Wilcox, J., 2017. CO2 capture from the industry sector. Prog. Energy Combust. Sci. 63, 146–172. https://doi.org/10.1016/j.pecs.2017.07.001.

Bernhardsen, I.M., Knuutila, H.K., June 2017. A review of potential amine solvents for CO_2 absorption process: Absorption capacity, cyclic capacity and pKa. Int. J. Greenh. Gas Control, 61 27–48.https://doi.org/10.1016/j.ijggc.2017.03.021.

Berstad, D., Anantharaman, R., Nekså, P., 2013. Low-temperature CO2 capture technologies – applications and potential. Int. J. Refrig. 36, 1403–1416. https://doi.org/10.1016/j.ijrefrig.2013.03.017.

Bisotti, F., Anders Hoff, K., Mathisen, A., Hovland, J., 2023. Direct air capture (DAC) deployment: national context cannot be neglected. A case study applied to Norway. Chem. Eng. Sci., 119313 https://doi.org/10.1016/j.ces.2023.119313.

Bisotti, F., Hoff, K.A., Mathisen, A., Hovland, J., 2024. Direct Air capture (DAC) deployment: a review of the industrial deployment. Chem. Eng. Sci. 283, 119416 https://doi.org/10.1016/j.ces.2023.119416.

Brigman, N., Shah, M.I., Falk-Pedersen, O., Cents, T., Smith, V., De Cazenove, T., Morken, A.K., Hvidsten, O.A., Chhaganlal, M., Feste, J.K., Lombardo, G., Bade, O.M., Knudsen, J., Subramoney, S.C., Fostås, B.F., De Koeijer, G., Hamborg, E.S., 2014. Results of Amine Plant Operations from 30 Wt% and 40 Wt% Aqueous MEA Testing at the CO2 Technology Centre Mongstad. Elsevier Ltd, pp. 6012–6022. https://doi.org/10.1016/j.egypro.2014.11.635.

Buchner, G.A., Stepputat, K.J., Zimmermann, A.W., Schomäcker, R., 2019. Specifying technology readiness levels for the chemical industry. Ind. Eng. Chem. Res. 58, 6957–6969. https://doi.org/10.1021/acs.iecr.8b05693.

Bui, M., Adjiman, C.S., Bardow, A., Anthony, E.J., Boston, A., Brown, S., Fennell, P.S., Fuss, S., Galindo, A., Hackett, L.A., Hallett, J.P., Herzog, H.J., Jackson, G., Kemper, J., Krevor, S., Maitland, G.C., Matuszewski, M., Metcalfe, I.S., Petit, C., Puxty, G., Reimer, J., Reiner, D.M., Rubin, E.S., Scott, S.A., Shah, N., Smit, B., Trusler, J.P.M., Webley, P., Wilcox, J., Mac Dowell, N., 2018. Carbon capture and storage (CCS): the way forward. Energy Environ. Sci. 11, 1062–1176. https://doi.org/10.1039/C7EE02342A.

Bui, M., Flø, N.E., de Cazenove, T., Mac Dowell, N., 2020. Demonstrating flexible operation of the Technology Centre Mongstad (TCM) CO2 capture plant. Int. J. Greenh. Gas Control 93, 102879. https://doi.org/10.1016/j.ijggc.2019.102879.

Buvik, V., Høisæter, K.K., Vevelstad, S.J., Knuutila, H.K., 2021. A review of degradation and emissions in post-combustion CO2 capture pilot plants. Int. J. Greenh. Gas Control 106. https://doi.org/10.1016/j.ijggc.2020.103246, 103246–103246.

Buzzi-Ferraris, G., Manenti, F., 2011. Data interpretation and correlation. In: Kirk-Othmer Encyclopedia of Chemical Technology, pp. 1–33. https://doi.org/10.1002/0471238961.databuzz.a01.
Cachola, C. da S., Ciotta, M., Azevedo dos Santos, A., Peyerl, D., 2023. Deploying of the carbon capture technologies for CO2 emission mitigation in the industrial sectors. Carbon Capture Sci. Technol. 7 https://doi.org/10.1016/j.ccst.2023.100102.
Chen, Guangying, Chen, Guangjie, Peruzzini, M., Zhang, R., Barzagli, F., 2022. Understanding the potential benefits of blended ternary amine systems for CO2 capture processes through 13C NMR speciation study and energy cost analysis. Separ. Purif. Technol. 291, 120939 https://doi.org/10.1016/j.seppur.2022.120939.
Chinen, A.S., Morgan, J.C., Omell, B., Bhattacharyya, D., Miller, D.C., 2019. Dynamic data reconciliation and validation of a dynamic model for solvent-based CO2 capture using pilot-plant data. Ind. Eng. Chem. Res. 58, 1978–1993. https://doi.org/10.1021/acs.iecr.8b04489.
Conway, W., Yang, Q., James, S., Wei, C.-C., Bown, M., Feron, P., Puxty, G., 2014. Designer amines for post combustion CO2 capture processes. Energy Proc. 63, 1827–1834. https://doi.org/10.1016/j.egypro.2014.11.190.
Costelloe, B., Finn, D., 2003. Indirect evaporative cooling potential in air–water systems in temperate climates. Energy Build. 35, 573–591. https://doi.org/10.1016/S0378-7788(02)00161-5.
Cruz, M. de A., Brigagão, G.V., de Medeiros, J.L., Musse, A.P.S., Kami, E., Freire, R.L.A., Araújo, O. de Q.F., 2023. Decarbonization of energy supply to offshore oil & gas production with post-combustion capture: a simulation-based techno-economic analysis. Energy 274, 127349. https://doi.org/10.1016/j.energy.2023.127349.
Demonstrating a Refinery-Adapted Cluster-Integrated Strategy to Enable Full-Chain CCUS Implementation | REALISE Project | Fact Sheet | H2020, 2020. CORDIS | European Commission [WWW Document]. https://cordis.europa.eu/project/id/884266, 1.16.24.
Dutcher, B., Fan, M., Russell, A.G., 2015. Amine-based CO2 capture technology development from the beginning of 2013-A review. ACS Appl. Mater. Interfaces 7, 2137–2148. https://doi.org/10.1021/am507465f.
Edwards, T.J., Maurer, G., Newman, J., Prausnitz, J.M., 1978. Vapor-liquid equilibria in multicomponent aqueous solutions of volatile weak electrolytes. AIChE J. 24, 966–976. https://doi.org/10.1002/aic.690240605.
El Hadri, N., Quang, D.V., Goetheer, E.L.V., Abu Zahra, M.R.M., 2017. Aqueous amine solution characterization for post-combustion CO2 capture process. Appl. Energy 185, 1433–1449. https://doi.org/10.1016/j.apenergy.2016.03.043.
Elliott, W., Benz, A., Gibbins, J., Michailos, S., 2022. An open-access FEED study for a post-combustion CO2 capture plant retrofit to a CCGT. SSRN J. https://doi.org/10.2139/ssrn.4286280.
Emissions Gap Report 2022, 2022. UNEP - UN Environment Programme [WWW Document]. http://www.unep.org/resources/emissions-gap-report-2022, 4.25.23.
Feron, P.H.M., Cousins, A., Jiang, K., Zhai, R., Garcia, M., 2020. An update of the benchmark post-combustion CO2-capture technology. Fuel 273, 117776. https://doi.org/10.1016/j.fuel.2020.117776.
Flagiello, D., Parisi, A., Lancia, A., Di Natale, F., 2021. A review on gas-liquid mass transfer coefficients in packed-bed columns. ChemEngineering 5. https://doi.org/10.3390/chemengineering5030043.
Fostås, B., Gangstad, A., Nenseter, B., Pedersen, S., Sjøvoll, M., Sørensen, A.L., 2011. Effects of NOx in the flue gas degradation of MEA. Energy Proc. 4, 1566–1573. https://doi.org/10.1016/j.egypro.2011.02.026.
Gabrielsen, J., Svendsen, H.F., Michelsen, M.L., Stenby, E.H., Kontogeorgis, G.M., 2007. Experimental validation of a rate-based model for CO2 capture using an AMP solution. Chem. Eng. Sci. 62, 2397–2413. https://doi.org/10.1016/j.ces.2007.01.034.
Gao, T., Rochelle, G.T., 2020. CO2 absorption from gas turbine flue gas by aqueous piperazine with intercooling. Ind. Eng. Chem. Res. 59, 7174–7181. https://doi.org/10.1021/acs.iecr.9b05733.
Ghilardi, A., 2020. Innovative Solvents for Carbon Capture : Diethylethanolamine (DEEA) and its Blend with N-Methyl-1,3-Diaminopropane (MAPA) [WWW Document]. URL. https://www.politesi.polimi.it/handle/10589/169265?mode=complete, 1.16.24.
Gilardi, M., Bisotti, F., Tobiesen, A., Knuutila, H.K., Bonalumi, D., 2023. An approach for VLE model development, validation, and implementation in Aspen Plus for amine blends in CO2 capture: the HS3 solvent case study. Int. J. Greenh. Gas Control 126, 103911. https://doi.org/10.1016/j.ijggc.2023.103911.
Gilardi, M., Bonalumi, D., Moioli, S., 2022. Process design for the treatment of the irving oil refinery flue gas: heat recovery, energy analysis and CO2 capture. SSRN J. https://doi.org/10.2139/ssrn.4285555.
Hartono, A., Ahmad, R., Svendsen, H.F., Knuutila, H.K., 2021. New solubility and heat of absorption data for CO2 in blends of 2-amino-2-methyl-1-propanol (AMP) and Piperazine (PZ) and a new eNRTL model representation. Fluid Phase Equil. 550 https://doi.org/10.1016/j.fluid.2021.113235.
Hartono, A., Knuutila, H.K., 2023. Densities, viscosities of pure 1-(2-hydroxyethyl) pyrrolidine, 3-amino-1-propanol, water, and their mixtures at 293.15 to 363.15 K and atmospheric pressure. J. Chem. Eng. Data 68, 525–535. https://doi.org/10.1021/acs.jced.2c00648.
Hartono, A., Knuutila, H.K., 2021. Optimum solvent concentration to lower energy demands for CO2 capture in refinery cases. SSRN J. https://doi.org/10.2139/ssrn.3814859.
Hartono, A., Rennemo, R., Awais, M., Vevelstad, S.J., Brakstad, O.G., Kim, I., Knuutila, H.K., 2017. Characterization of 2-piperidineethanol and 1-(2-hydroxyethyl)pyrrolidine as strong bicarbonate forming solvents for CO2 capture. Int. J. Greenh. Gas Control 63, 260–271. https://doi.org/10.1016/j.ijggc.2017.05.021.
Hartono, A., Vevelstad, S.J., Ciftja, A., Knuutila, H.K., 2017. Screening of strong bicarbonate forming solvents for CO2 capture. Int. J. Greenh. Gas Control 58, 201–211. https://doi.org/10.1016/j.ijggc.2016.12.018.
Henni, A., Li, J., Tontiwachwuthikul, P., 2008. Reaction kinetics of CO2 in aqueous 1-amino-2-propanol, 3-amino-1-propanol, and dimethylmonoethanolamine solutions in the temperature range of 298-313 K using the stopped-flow technique. Ind. Eng. Chem. Res. 47, 2213–2220. https://doi.org/10.1021/ie070587r.
Hetland, J., Kvamsdal, H.M., Haugen, G., Major, F., Kårstad, V., Tjellander, G., 2009. Integrating a full carbon capture scheme onto a 450MWe NGCC electric power generation hub for offshore operations: presenting the Sevan GTW concept. Appl. Energy 86, 2298–2307. https://doi.org/10.1016/j.apenergy.2009.03.019.
High Performance Capture - HiPerCap | HIPERCAP Project | Fact Sheet | FP7 | CORDIS | European Commission [WWW Document], n.d. URL https://cordis.europa.eu/project/id/608555 (accessed 5.8.23).
Horvath, A.L., 1985. Handbook of Aqueous Electrolyte Solutions: Physical Properties, Estimation and Correlation Methods. Ellis Horwood series in physical chemistry. Ellis Horwood.
Khakharia, P., Huizinga, A., Jurado Lopez, C., Sanchez Sanchez, C., de Miguel Mercader, F., Vlugt, T.J.H., Goetheer, E., 2014. Acid wash scrubbing as a countermeasure for ammonia emissions from a postcombustion CO2 capture plant. Ind. Eng. Chem. Res. 53, 13195–13204. https://doi.org/10.1021/ie502045c.
Kim, I., Vevelstad, S.J., Knuutila, H.K., Hartono, A., Haugen, G., Tobiesen, A., Irons, R., Drew, R., Kvamsdal, H.M., 2019. Solvent technology development in the EU project HiPerCap: from molecular simulation to technological roadmap for large scale demonstration. SSRN J. https://doi.org/10.2139/ssrn.3365947.
Knuutila, H.K., Rennemo, R., Ciftja, A.F., 2019. New solvent blends for post-combustion CO2 capture. Green Energy Environ. 4, 439–452. https://doi.org/10.1016/j.gee.2019.01.007.
Kvamsdal, H.M., Ehlers, S., Kather, A., Khakharia, P., Nienoord, M., Fosbøl, P.L., 2016. Optimizing integrated reference cases in the OCTAVIUS project. Int. J. Greenh. Gas Control 50, 23–36. https://doi.org/10.1016/j.ijggc.2016.04.012.
Kvamsdal, H.M., Haugen, G., Brown, J., Wolbers, P., Drew, R.J., Khakharia, P., Monteiro, J.G.M.-S., Goetheer, E.L.V., Middelkamp, J., Kanniche, M., Sirvent, A.J., 2017. Reference case and test case for benchmarking of HiPerCap technologies. Energy Proc. 114, 2642–2657. https://doi.org/10.1016/j.egypro.2017.03.1448.
Kvamsdal, H.M., Kim, I., Van Os, P., Pevida, C., Hägg, M.-B., Brown, J., Robinson, L., Feron, P., 2014. HiPerCap: a new FP7 project for development and assessment of novel and emerging post-combustion CO2 capture technologies. Energy Proc. 63, 6166–6172. https://doi.org/10.1016/j.egypro.2014.11.648.
Kvamsdal, H.M., Rochelle, G.T., 2008. Effects of the temperature bulge in CO2 absorption from flue gas by aqueous monoethanolamine. Ind. Eng. Chem. Res. 47, 867–875. https://doi.org/10.1021/ie061651s.
Lassauce, A., Alix, P., Raynal, L., Royon-Lebeaud, A., Haroun, Y., 2014. Pressure drop, capacity and mass transfer area requirements for post-combustion carbon capture by solvents. Oil Gas Sci. Technol. – Rev. IFP Energies nouvelles 69, 1021–1034. https://doi.org/10.2516/ogst/2013154.
Lawal, A., Wang, M., Stephenson, P., Obi, O., 2012. Demonstrating full-scale post-combustion CO2 capture for coal-fired power plants through dynamic modelling and simulation. Fuel 101, 115–128. https://doi.org/10.1016/j.fuel.2010.10.056.
Lee, J., Kim, J., Kim, H., Lee, K.S., Won, W., 2019. A new modeling approach for a CO2 capture process based on a blended amine solvent. J. Nat. Gas Sci. Eng. 61, 206–214. https://doi.org/10.1016/j.jngse.2018.11.020.
Lee, M.Y., 2022. Mass transfer technology for next-generation carbon capture. SSRN J. https://doi.org/10.2139/ssrn.4298263.
Li, K., Cousins, A., Yu, H., Feron, P., Tade, M., Luo, W., Chen, J., 2016. Systematic study of aqueous monoethanolamine-based CO2 capture process: model development and process improvement. Energy Sci. Eng. 4, 23–39. https://doi.org/10.1002/ese3.101.
Liang, Z. (Henry), Rongwong, W., Liu, H., Fu, K., Gao, H., Cao, F., Zhang, R., Sema, T., Henni, A., Sumon, K., Nath, D., Gelowitz, D., Srisang, W., Saiwan, C., Benamor, A., Al-Marri, M., Shi, H., Supap, T., Chan, C., Zhou, Q., Abu-Zahra, M., Wilson, M., Olson, W., Idem, R., Tontiwachwuthikul, P.(P.T.), 2015. Recent progress and new developments in post-combustion carbon-capture technology with amine based solvents. Int. J. Greenh. Gas Control 40, 26–54. https://doi.org/10.1016/j.ijggc.2015.06.017.
Lin, Y., ten Kate, A., Mooijer, M., Delgado, J., Fosbøl, P.L., Thomsen, K., 2010. Comparison of activity coefficient models for electrolyte systems. AIChE J. 56, 1334–1351. https://doi.org/10.1002/aic.12040.
Linnenberg, S., Darde, V., Oexmann, J., Kather, A., van Well, W.J.M., Thomsen, K., 2012. Evaluating the impact of an ammonia-based post-combustion CO2 capture process on a steam power plant with different cooling water temperatures. Int. J. Greenh. Gas Control 10, 1–14. https://doi.org/10.1016/j.ijggc.2012.05.003.
Liu, H., Li, M., Idem, R., Tontiwachwuthikul, P.(P.T.), Liang, Z., 2017. Analysis of solubility, absorption heat and kinetics of CO2 absorption into 1-(2-hydroxyethyl) pyrrolidine solvent. Chem. Eng. Sci. 162, 120–130. https://doi.org/10.1016/j.ces.2016.12.070.
Lu, R., Li, K., Chen, J., Yu, H., Tade, M., 2017. CO2 capture using piperazine-promoted, aqueous ammonia solution: rate-based modelling and process simulation. Int. J. Greenh. Gas Control 65, 65–75. https://doi.org/10.1016/j.ijggc.2017.08.018.
Luo, X., Wang, M., 2017. Improving prediction accuracy of a rate-based model of an MEA-based carbon capture process for large-scale commercial deployment. Engineering 3, 232–243. https://doi.org/10.1016/J.ENG.2017.02.001.
Madeddu, C., Errico, M., Baratti, R., 2018. Process analysis for the carbon dioxide chemical absorption–regeneration system. Appl. Energy 215, 532–542. https://doi.org/10.1016/j.apenergy.2018.02.033.

Mantripragada, H.C., Zhai, H., Rubin, E.S., 2019. Boundary Dam or Petra Nova – which is a better model for CCS energy supply? Int. J. Greenh. Gas Control 82, 59–68. https://doi.org/10.1016/j.ijggc.2019.01.004.

Markewitz, P., Kuckshinrichs, W., Leitner, W., Linssen, J., Zapp, P., Bongartz, R., Schreiber, A., Müller, T.E., 2012. Worldwide innovations in the development of carbon capture technologies and the utilization of CO2. Energy Environ. Sci. 5, 7281–7305. https://doi.org/10.1039/C2EE03403D.

Mejdell, T., Kvamsdal, H.M., Hauger, S.O., Gjertsen, F., Tobiesen, F.A., Hillestad, M., 2022. Demonstration of non-linear model predictive control for optimal flexible operation of a CO2 capture plant. Int. J. Greenh. Gas Control 117, 103645. https://doi.org/10.1016/j.ijggc.2022.103645.

Mejdell, T., Vassbotn, T., Juliussen, O., Tobiesen, A., Einbu, A., Knuutila, H., Hoff, K.A., Andersson, V., Svendsen, H.F., 2011. Novel full height pilot plant for solvent development and model validation. Energy Proc. 4, 1753–1760. https://doi.org/10.1016/j.egypro.2011.02.050.

Meng, F., Meng, Y., Ju, T., Han, S., Lin, L., Jiang, J., 2022. Research progress of aqueous amine solution for CO2 capture: a review. Renew. Sustain. Energy Rev. 168, 112902 https://doi.org/10.1016/j.rser.2022.112902.

Michailos, S., Gibbins, J., 2022. A modelling study of post-combustion capture plant process conditions to facilitate 95–99% CO2 capture levels from gas turbine flue gases. Front. Energy Res. 10, 866838 https://doi.org/10.3389/fenrg.2022.866838.

Montañés, R.M., Flø, N.E., Dutta, R., Nord, L.O., Bolland, O., 2017. Dynamic Process Model Development and Validation with Transient Plant Data Collected from an MEA Test Campaign at the CO2 Technology Center Mongstad. Elsevier Ltd, pp. 1538–1550. https://doi.org/10.1016/j.egypro.2017.03.1284.

Morgan, J., Campbell, M., Putta, K., Shah, M.I., Matuszewski, M., Omell, B., 2022. Development of process model of CESAR1 solvent system and validation with large pilot data. SSRN J. https://doi.org/10.2139/ssrn.4276820.

Morgan, J.C., Soares Chinen, A., Omell, B., Bhattacharyya, D., Tong, C., Miller, D.C., Buschle, B., Lucquiaud, M., 2018. Development of a rigorous modeling framework for solvent-based CO2 capture. Part 2: steady-state validation and uncertainty quantification with pilot plant data. Ind. Eng. Chem. Res. 57, 10464–10481. https://doi.org/10.1021/acs.iecr.8b01472.

Moser, P., Wiechers, G., Schmidt, S., Monteiro, J.G.M.-S., Goetheer, E., Charalambous, C., Saleh, A., van der Spek, M., Garcia, S., 2021. ALIGN-CCUS: results of the 18-month test with aqueous AMP/PZ solvent at the pilot plant at Niederaussem – solvent management, emissions and dynamic behavior. Int. J. Greenh. Gas Control 109, 103381. https://doi.org/10.1016/j.ijggc.2021.103381.

Mudhasakul, S., Ku, H., Douglas, P.L., 2013. A simulation model of a CO2 absorption process with methyldiethanolamine solvent and piperazine as an activator. Int. J. Greenh. Gas Control 15, 134–141. https://doi.org/10.1016/j.ijggc.2013.01.023.

Nessi, E., Papadopoulos, A.I., Seferlis, P., 2021. A review of research facilities, pilot and commercial plants for solvent-based post-combustion CO2 capture: packed bed, phase-change and rotating processes. Int. J. Greenh. Gas Control 111, 103474. https://doi.org/10.1016/j.ijggc.2021.103474.

Neveux, T., Le Moullec, Y., Corriou, J.-P., Favre, E., 2013. Modeling CO2 capture in amine solvents: prediction of performance and insights on limiting phenomena. Ind. Eng. Chem. Res. 52, 4266–4279. https://doi.org/10.1021/ie302768s.

Nookuea, W., Tan, Y., Li, H., Thorin, E., Yan, J., 2016. Impacts of thermo-physical properties of gas and liquid phases on design of absorber for CO2 capture using monoethanolamine. Int. J. Greenh. Gas Control 52, 190–200. https://doi.org/10.1016/j.ijggc.2016.07.012.

Oexmann, J., Kather, A., Linnenberg, S., Liebenthal, U., 2012. Post-combustion CO2 capture: chemical absorption processes in coal-fired steam power plants. Greenhouse Gases: Sci. Technol. 2, 80–98. https://doi.org/10.1002/ghg.1273.

Park, K., Øi, L.E., 2017. Optimization of Gas Velocity and Pressure Drop in CO2 Absorption Column, pp. 292–297. https://doi.org/10.3384/ecp17138292.

Pellegrini, L.A., Gilardi, M., Giudici, F., Spatolisano, E., 2021. New solvents for co2 and h2s removal from gaseous streams. Energies 14. https://doi.org/10.3390/en14206687.

Pellegrini, L.A., Langè, S., Baccanelli, M., De Guido, G., 2015. Techno-Economic Analysis of LNG Production Using Cryogenic vs Conventional Techniques for Natural Gas Purification. OMC, pp. 2015–2330.

Penny, D.E., Ritter, T.J., 1983. Kinetic study of the reaction between carbon dioxide and primary amines. J. Chem. Soc., Faraday Trans. 1 79, 2103–2109. https://doi.org/10.1039/F19837902103.

Pinsent, B.R.W., Pearson, L., Roughton, F.J.W., 1956. The kinetics of combination of carbon dioxide with hydroxide ions. Trans. Faraday Soc. 52, 1512–1520. https://doi.org/10.1039/TF9565201512.

Plaza, J.M., Wagener, D.V., Rochelle, G.T., 2009. Modeling CO2 capture with aqueous monoethanolamine. Energy Proc. 1, 1171–1178. https://doi.org/10.1016/j.egypro.2009.01.154.

Poling, B.E., Prausnitz, J.M., O'Connell, J.P., 2001. Properties of Gases and Liquids, fifth ed. McGraw-Hill Education, New York.

Putta, K.R., Svendsen, H.F., Knuutila, H.K., 2017. Study of the effect of condensation and evaporation of water on heat and mass transfer in CO2 absorption column. Chem. Eng. Sci. 172, 353–369. https://doi.org/10.1016/j.ces.2017.06.037.

Raynal, L., Bouillon, P.A., Gomez, A., Broutin, P., 2011. From MEA to demixing solvents and future steps, a roadmap for lowering the cost of post-combustion carbon capture. Chem. Eng. J. 171, 742–752. https://doi.org/10.1016/j.cej.2011.01.008.

Razi, N., Bolland, O., Svendsen, H., 2012. Review of design correlations for CO2 absorption into MEA using structured packings. Int. J. Greenh. Gas Control 9, 193–219. https://doi.org/10.1016/j.ijggc.2012.03.003.

Renon, H., Prausnitz, J.M., 1969. Estimation of parameters for the NRTL equation for excess gibbs energies of strongly nonideal liquid mixtures. Ind. Eng. Chem. Process Des. Dev. 8, 413–419. https://doi.org/10.1021/i260031a019.

Rosha, P., Ibrahim, H., 2023. Hydrogen production via solid waste gasification with subsequent amine-based carbon dioxide removal using Aspen Plus. Int. J. Hydrogen Energy 48, 24607–24618. https://doi.org/10.1016/j.ijhydene.2022.07.103.

Schiffhauer, M., Veitch, C., 2009. Increasing Natural Gas Boiler Efficiency by Capturing Waste Energy from Flue Gas.

Seider, W.D., Lewin, D.R., Seader, J.D., Widagdo, S., Gani, R., 2017. Chapter 6, heuristics for process synthesis. In: Product and Process Design Principles: Synthesis, Analysis and Evaluation. John Wiley & Sons, pp. 132–162.

SEPA (Scottish Environment Protection Agency), 2015. Review of Amine Emissions from Carbon Capture Systems, pp. 1–86.

Shah, M.I., Lombardo, G., Fostås, B., Benquet, C., Kolstad Morken, A., De Cazenove, T., 2018. CO 2 Capture from RFCC Flue Gas with 30 Wt% MEA at Technology Centre Mongstad, Process Optimization and Performance Comparison.

Shatskikh, Y.V., Sharapov, A.I., Byankin, I.G., 2017. Analysis of deep heat recovery from flue gases. J. Phys. Conf. 891, 012188 https://doi.org/10.1088/1742-6596/891/1/012188.

Szulc, P., Tietze, T., Smykowski, D., 2018. The impact of the condensation process on the degree of cleaning of flue gases from acidic compounds. E3S Web Conf. 46, 00031 https://doi.org/10.1051/e3sconf/20184600031.

Tan, Y., Nookuea, W., Li, H., Thorin, E., Yan, J., 2016. Property impacts on carbon capture and storage (CCS) processes: a review. Energy Convers. Manag. 118, 204–222. https://doi.org/10.1016/j.enconman.2016.03.079.

Tobiesen, F.A., Haugen, G., Kim, I., Kvamsdal, H., 2017. Simulation and energy evaluation of two novel solvents developed in the EU project HiPerCap. Energy procedia, 13th international conference on greenhouse gas control technologies. GHGT-13 114, 1621–1629. https://doi.org/10.1016/j.egypro.2017.03.1291, 14-18 November 2016, Lausanne, Switzerland.

Tsay, C., Pattison, R.C., Zhang, Y., Rochelle, G.T., Baldea, M., 2019. Rate-based modeling and economic optimization of next-generation amine-based carbon capture plants. Appl. Energy 252, 113379. https://doi.org/10.1016/j.apenergy.2019.113379.

Van Wagener, D.H., Rochelle, G.T., 2011. Stripper configurations for CO2 capture by aqueous monoethanolamine. Chem. Eng. Res. Des. 89, 1639–1646. https://doi.org/10.1016/j.cherd.2010.11.011.

Vevelstad, S.J., Grimstvedt, A., François, M., Knuutila, H.K., Haugen, G., Wiig, M., Vernstad, K., 2023. Chemical stability and characterization of degradation products of blends of 1-(2-hydroxyethyl)pyrrolidine and 3-Amino-1-propanol. Ind. Eng. Chem. Res. 62, 610–626. https://doi.org/10.1021/acs.iecr.2c03068.

Wang, C., Seibert, A.F., Rochelle, G.T., 2015. Packing characterization: absorber economic analysis. Int. J. Greenh. Gas Control 42, 124–131. https://doi.org/10.1016/j.ijggc.2015.07.027.

Wang, T., Hovland, J., Jens, K.J., 2015. Amine reclaiming technologies in post-combustion carbon dioxide capture. J. Environ. Sci. 27, 276–289. https://doi.org/10.1016/j.jes.2014.06.037.

Zhai, H., Rubin, E.S., Versteeg, P.L., 2011. Water use at pulverized coal power plants with postcombustion carbon capture and storage. Environ. Sci. Technol. 45, 2479–2485. https://doi.org/10.1021/es1034443.

Zhang, R., Li, Y., He, X., Niu, Y., Li, C., Amer, M.W., Barzagli, F., 2023a. Investigation of the improvement of the CO2 capture performance of aqueous amine sorbents by switching from dual-amine to trio-amine systems. Separ. Purif. Technol. 316, 123810 https://doi.org/10.1016/j.seppur.2023.123810.

Zhang, R., Liu, H., Liu, R., Niu, Y., Yang, L., Barzagli, F., Li, C., Xiao, M., 2023b. Speciation and gas-liquid equilibrium study of CO2 absorption in aqueous MEA-DEEA blends. Gas Sci. Eng. 119, 205135 https://doi.org/10.1016/j.jgsce.2023.205135.

Zhang, S., Lu, Y., 2015. Kinetic performance of CO2 absorption into a potassium carbonate solution promoted with the enzyme carbonic anhydrase: comparison with a monoethanolamine solution. Chem. Eng. J. 279, 335–343. https://doi.org/10.1016/j.cej.2015.05.034.

Zhang, Y., Chen, H., Chen, C.-C., Plaza, J.M., Dugas, R., Rochelle, G.T., 2009. Rate-based process modeling study of CO2 capture with aqueous monoethanolamine solution. Ind. Eng. Chem. Res. 48, 9233–9246. https://doi.org/10.1021/ie900068k.